AD-A176 755 PARTICLE SIZING IN A SOLID PROPELLANT ROCKET MOTOR USING A LIGHT SCATTERING TECHNIQUE(U) NAVAL POSTGRADUATE SCHOOL MONTEREY CA M G KEITH DEC 86 1/1

UNCLASSIFIED F/G 21/2 NL

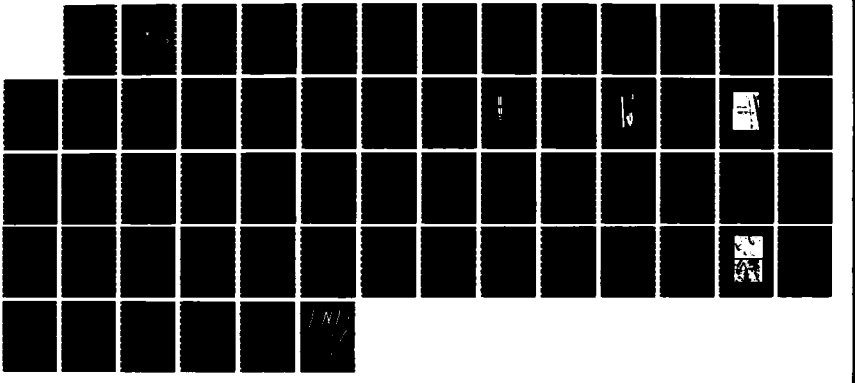

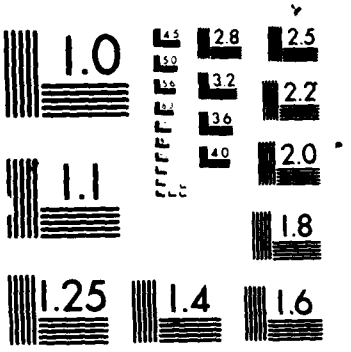

# NAVAL POSTGRADUATE SCHOOL
## Monterey, California




# THESIS

PARTICLE SIZING IN A SOLID PROPELLANT ROCKET MOTOR USING A LIGHT SCATTERING TECHNIQUE

by

Michael G. Keith

December 1986

Thesis Advisor: D. W. Netzer

Approved for public release; distribution is unlimited

SECURITY CLASSIFICATION OF THIS PAGE

# REPORT DOCUMENTATION PAGE

| | |
|---|---|
| 1a REPORT SECURITY CLASSIFICATION<br>Unclassified | 1b RESTRICTIVE MARKINGS |
| 2a SECURITY CLASSIFICATION AUTHORITY | 3 DISTRIBUTION/AVAILABILITY OF REPORT<br>Approved for public release; distribution is unlimited |
| 2b DECLASSIFICATION/DOWNGRADING SCHEDULE | |
| 4 PERFORMING ORGANIZATION REPORT NUMBER(S) | 5 MONITORING ORGANIZATION REPORT NUMBER(S) |
| 6a NAME OF PERFORMING ORGANIZATION<br>Naval Postgraduate School<br>6b OFFICE SYMBOL (If applicable)<br>67 | 7a NAME OF MONITORING ORGANIZATION<br>Naval Postgraduate School |
| 6c ADDRESS (City, State, and ZIP Code)<br>Monterey, California 93943-5000 | 7b ADDRESS (City, State, and ZIP Code)<br>Monterey, California 93943-5000 |
| 8a NAME OF FUNDING/SPONSORING ORGANIZATION<br>Air Force Rocket Propulsion Laboratory<br>8b OFFICE SYMBOL (If applicable) | 9 PROCUREMENT INSTRUMENT IDENTIFICATION NUMBER |
| 8c ADDRESS (City, State, and ZIP Code)<br>Edwards Air Force Base<br>California 93523 | 10 SOURCE OF FUNDING NUMBERS<br>PROGRAM ELEMENT NO<br>PROJECT NO F04611-86-X-0008<br>TASK NO<br>WORK UNIT ACCESSION NO |

11 TITLE (Include Security Classification)
PARTICLE SIZING IN A SOLID PROPELLANT ROCKET MOTOR USING A LIGHT SCATTERING TECHNIQUE

12 PERSONAL AUTHOR(S)
Keith, Michael G.

| 13a TYPE OF REPORT | 13b TIME COVERED | 14 DATE OF REPORT (Year, Month, Day) | 15 PAGE COUNT |
|---|---|---|---|
| Master's Thesis | FROM _____ TO _____ | 1986 December | 59 |

16 SUPPLEMENTARY NOTATION

| 17 COSATI CODES | | |
|---|---|---|
| FIELD | GROUP | SUB-GROUP |
| | | |
| | | |

18 SUBJECT TERMS (Continue on reverse if necessary and identify by block number)
Solid propellant; rocket motor; light scattering; particle sizing

19 ABSTRACT (Continue on reverse if necessary and identify by block number)

Research was conducted to determine particle sizes across the nozzle of a small solid propellant rocket motor. Particle size was determined using light scattering techniques. The present optical components limit the lower measurable particle size to approximately three microns. During the investigation, spurious light was detected in the motor optical path. It was determined that transient pressure gradients in the motor during motor pressure rise resulted in deflection of the laser beam. Neutral burning propellant grains were shown to eliminate most of the observed difficulty. The use of a ring array in place of the linear array in the motor cavity measurement system is suggested for system improvement.

| 20 DISTRIBUTION/AVAILABILITY OF ABSTRACT | 21 ABSTRACT SECURITY CLASSIFICATION | |
|---|---|---|
| ☒ UNCLASSIFIED/UNLIMITED ☐ SAME AS RPT ☐ DTIC USERS | Unclassified | |
| 22a NAME OF RESPONSIBLE INDIVIDUAL<br>D. W. Netzer | 22b TELEPHONE (Include Area Code)<br>(408) 646-2980 | 22c OFFICE SYMBOL<br>Code 67 Nt |

DD FORM 1473, 84 MAR 83 APR edition may be used until exhausted
All other editions are obsolete

SECURITY CLASSIFICATION OF THIS PAGE

Approved for public release; distribution is unlimited

# Particle Sizing in a Solid Propellant Rocket Motor Using a Light Scattering Technique

by

Michael G. Keith
Lieutenant Commander, United States Navy
B. S., United States Naval Academy, 1972
M. S., University of West Florida, 1974

Submitted in partial fulfillment of the requirements for the degree of

MASTER OF SCIENCE IN AERONAUTICAL ENGINEERING

from the

NAVAL POSTGRADUATE SCHOOL
December 1986

Author: Michael G. Keith
Michael G. Keith

Approved by: D. W. Netzer
D. W. Netzer, Thesis Advisor

M. F. Platzer
M. F. Platzer, Chairman,
Department of Aeronautics

J. N. Dyer
J. N. Dyer,
Dean of Science and Engineering

## ABSTRACT

Research was conducted to determine particle sizes across the nozzle of a small solid propellant rocket motor. Particle size was determined using light scattering techniques. The present optical components limit the lower measurable particle size to approximately three microns. During the investigation, spurious light was detected in the motor optical path. It was determined that transient pressure gradients in the motor during motor pressure rise resulted in deflection of the laser beam. Neutral burning propellant grains were shown to eliminate most of the observed difficulty. The use of a ring array in place of the linear array in the motor cavity measurement system is suggested for system improvement.

TABLE OF CONTENTS

LIST OF TABLES

LIST OF FIGURES

ACKNOWLEDGEMENTS

I would like to thank Professor D. W. Netzer for his unfailing support in the completion of this thesis.

# I. INTRODUCTION

This thesis was part of an ongoing investigation at the Naval Postgraduate School to determine particle sizes within the combustor and exhaust nozzle of solid propellant rocket motors. Several techniques are currently being used to obtain particle size, but primarily efforts have been directed toward holography and laser diffraction. Holography has been used to find the particle sizes as they leave the burning surface of the propellant. Laser diffraction has proven to be a viable method to measure particle size just prior to and aft of the rocket nozzle. Data is being gathered at all three locations to determine the various sizes of particles throughout their life cycle.

Particle size information is the most important parameter in accurate prediction of two phase flow losses. The particle size information is extremely difficult to obtain given the very high temperatures within the rocket and exhaust. Two phase flow losses are therefore somewhat unpredictable due to the lack of particle size data. This prevents computer models for rocket combustion performance from being as accurate as one would like [Ref. 1]. Additionally, particle size information is useful in studying combustor stability [Ref. 2]. The size distribution of the particles can play an important role in damping unwanted combustor pressure oscillations.

Various metals have long been used as fuel additives in solid propellant rockets to boost specific impulse. The most common metal used in rocket combustion is aluminum. The size of aluminum particles and the resulting aluminum oxide take on special significance with regard to two phase flow losses.

The specific light scattering technique in use at the Naval Postgraduate School is based upon the work of Buchele [Ref. 3]. This method is particularly well suited for rockets since it is a non-intrusive way to measure particle size within the motor environment. The method is insensitive to the refractive index of the particles and is independent of concentration over a considerable range. The size measurement obtained is the volume to surface mean diameter ($D_{32}$). The present study was limited to measuring $D_{32}$ between 1-50 microns, which favorably matches with the sizes of interest across the rocket nozzle for two phase flow losses.

The purposes of this thesis were to: (1) realign all the optics and record a "baseline" position for the light scattering apparatus to include light ray tracing diagrams, (2) determine the cause and correct an optical noise problem that existed in the motor laser beam path, (3) gather particle size data for a metallized propellant using a series of newly designed nozzles (The nozzles were designed to better simulate the flow through an actual full scale rocket), and (4) test a new particle injection system

designed to overcome the problems Horton [Ref. 4] had in getting particles to steadily drop from the head-end of the motor.

## II. THEORETICAL BACKGROUND

The complex scattering phenomena was first described by Mie in the form of equations involving Legendre polynomials and spherical Bessel functions. While these equations are still the most accurate way to describe scattering, investigations subsequent to Mie have found the equations to simplify when the scattering particle diameter is either considerably greater than or less than the wavelength of incident light. For particle diameters less than approximately 1/20th of the wavelength of light, the equations simplify to the Rayleigh approximation [Ref. 5]. For particle diameters somewhat greater than the wavelength of light, Fraunhofer diffraction dominates the scattering phenomena.

When a beam of light passes through a dispersion of non-absorbing particles the light is scattered by reflection, refraction, and diffraction. Reflection and refraction account for most of the wide angle scattering, while diffraction scattering accounts for most of the light scattered at small angles [Ref. 6]. The scattering at small angles takes place in what is called the main forward lobe. The main forward lobe is dominated by Fraunhofer diffraction and is therefore independent of the index of refraction.

In Fraunhofer diffraction, scattering is controlled by the particle size (diameter). One type of diameter that can

be calculated from measuring scattered light in the main forward lobe is $D_{32}$. The value of $D_{32}$ can be determined for a polydispersion of spherical particles to a good degree of accuracy for a wide range of distributions [Refs. 7 and 8].

$$D_{32} = \int_{\emptyset}^{D_{MAX}} N_r(D) D^3 dD \; / \int_{\emptyset}^{D_{MAX}} N_r(D) D^2 dD \qquad (1)$$

$N_r(D)$ is the particle size distribution function. The distribution of choice used in the present study was the Upper Limit Distribution Function (ULDF) for polydispersions. This distribution came from Mugele and Evans [Ref. 9] and includes the assumption that no particle exists with a diameter larger than approximately ten times $D_{32}$.

The light scattering method employed herein was introduced by Buchele [Ref. 3]. Light scattering intensity and particle diameter are related through the Fraunhofer diffraction formula. For a monodispersion with small forward scattering angles:

$$\frac{I(\Theta)}{I(0)} = \left[ \frac{2J_1(\alpha \Theta)}{\alpha \Theta} \right]^2 \qquad (2)$$

$I(\Theta)$ is the intensity of scattered light at a given angle ($\Theta$). $I(0)$ is the intensity of scattered light at theta equal to zero degrees. $J_1(\alpha \Theta)$ is the first order

Bessel function. $\alpha$ is the particle size parameter equal to $\pi D/\lambda$ where D is particle diameter and $\lambda$ is the wavelength of light.

For a polydispersion obeying the ULDF this equation can be closely approximated by a Gaussian curve, when $\alpha\theta \lesssim 3$, using the following expression:

$$\frac{I(\theta)}{I(0)} = \exp\left[-0.57\,\alpha\theta\right]^2 \qquad (3)$$

If the ratio of intensities at two angles is taken, the lower limit of particle diameter measurement is about one micron, on the order of the wavelength of light. The formula for the ratio at two angles follows:

$$\frac{I_2}{I_1} = \exp\left[-(0.57\ \pi D/\lambda\ )^2\ (\theta_2^2 - \theta_1^2)\right] \qquad (4)$$

Where $I_1$ is the intensity at $\theta_1$

$I_2$ is the intensity at $\theta_2$

Solving for diameter the expression becomes:

$$D^2 = -(\lambda/0.57\pi)^2 \ln(I_2/I_1)/(\theta_2^2-\theta_1^2) \qquad (5)$$

The upper limit on measuring D in the present apparatus was approximately 50 microns. This is determined by the increasing difficulty of measuring intensity of forward scattered light at angles less than one degree.

The following list summarizes the pertinent assumptions related to the light scattering measurements used in this investigation:

(1) Non-absorbing spheres

(2) Independence from refractive index

(3) Fraunhofer diffraction

(4) Gaussian approximation to Fraunhofer curve

(5) Polydispersion, upper limit distribution function

(6) $D_{32}$ independent of size distribution

(7) Independent scattering

# III. EXPERIMENTAL APPARATUS

## A. ROCKET MOTOR

The rocket motor is pictured in Figure 3.1. It was the same motor used by Horton [Ref. 4], however, three improvements were made. First, the small window (.15" diameter) was converted to a large window (.3" diameter). The purpose of the change was to decrease window edge and aperture effects. Second, a nitrogen injection system was added to the particle feeder to overcome particle drop problems encountered by Horton. Third, new contoured nozzles were constructed to decrease shocks and flow separation in the nozzle exhaust, thereby more closely approximating the flow in an actual rocket nozzle.

The rocket motor is shown in schematic form in Figure 3.2. Two types of propellant were used, the first a non-metallized propellant, X-55, consisting of 86% ammonium perchlorate and 14% HTPB. The second, a metallized propellant, UTP-19048, containing 2% aluminum. The ignition source for the propellant was a $BKNO_3$ igniter fired by electrically shorting an imbedded nickel filament.

The particle feeder with the new nitrogen injection system is pictured in Figure 3.3 and shown schematically in Figure 3.4. The nitrogen injection tube was inserted into the top of the particle feeder and the flow rate was

adjusted using a sonically choked needle valve. The mass flow of nitrogen represented less than 5% of the total mass flow through the rocket exhaust nozzle.

The specifications for the original nozzle and the new contoured nozzles are listed in Table I.

## B. LIGHT SCATTERING APPARATUS

The complete light scattering equipment with rocket in place is shown in Figure 3.5. The over and under arrangement of the motor and exhaust laser systems is seen in the photograph. The light sources used were two helium neon lasers. Specifications are given in Table II.

The light scattering apparatus is depicted schematically in Figure 3.6. The exhaust beam was initially processed through a spatial filter and collimating lens. The beam then penetrated the exhaust. After the exhaust the main beam was blocked to prevent saturation of the photodiodes. The scattered light from the test section entered a narrow pass filter and fell upon the objective lens. The objective lens had a focal length of 50 centimeters which focused the scattering profile on a photodiode array. The photodiode array was a Reticon G-series solid state scanning device consisting of 1024 photodiodes on 25 micron centers. The overall length of the array was approximately one inch. The laser that penetrated the motor used an arrangement similar to the exhaust beam.

Figures 3.7 through 3.10 represent the recorded "baseline" position for the light scattering apparatus including beam clearances and angles measured.

## C. DATA ACQUISITION AND REDUCTION

Data was acquired in accordance with the computer program by Harris [Ref. 10]. A Hewlett Packard HP9836S computer served as the system controller. Data was converted from analog to digital and stored in a HP6942A multiprogrammer. The computer was preprogrammed to begin taking data when the motor reached a given pressure, typically 180 psi. At that time, voltages from the scanning photodiodes were stored sequentially. Eight scans of the motor photodiode array were stored followed by four scans of the exhaust photodiode array. Scans were limited by the amount of available storage. The total time to record all 12 scans was less than one-half second.

The data was reduced in accordance with the computer program by Rosa [Ref. 11]. The multiple photodiode scans were averaged and the resultant scan was plotted on a graph of voltage (intensity, I) versus photodiode number (or angle, $\Theta$). This experimentally obtained curve was compared to the theoretical curve generated from the Gaussian approximation:

$$\frac{I_2}{I_1} = \exp\left[-(0.57\,\pi D/\lambda)^2(\Theta_2^2-\Theta_1^2)\right]$$

The theoretical curve was then generated for different values of $D_{32}$ interactively at the computer terminal until the theoretical curve and experimental curve coincided. The initial values for $I_1$ and $\Theta_1$ were chosen from a point on the experimentally obtained profile. This curve fitting process determined the value of $D_{32}$.

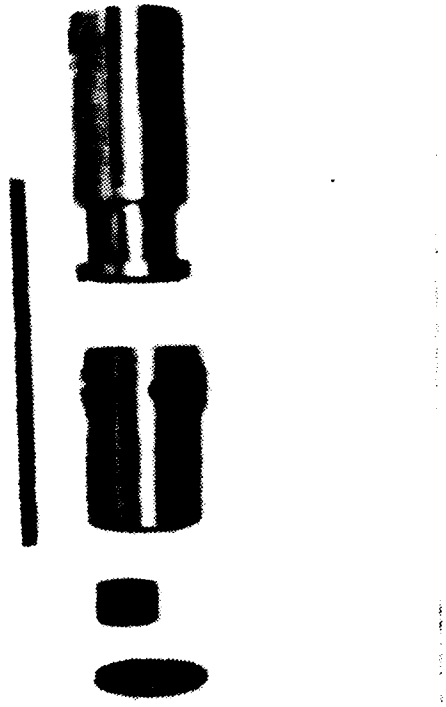


Figure 3.1 Photograph of Rocket Motor

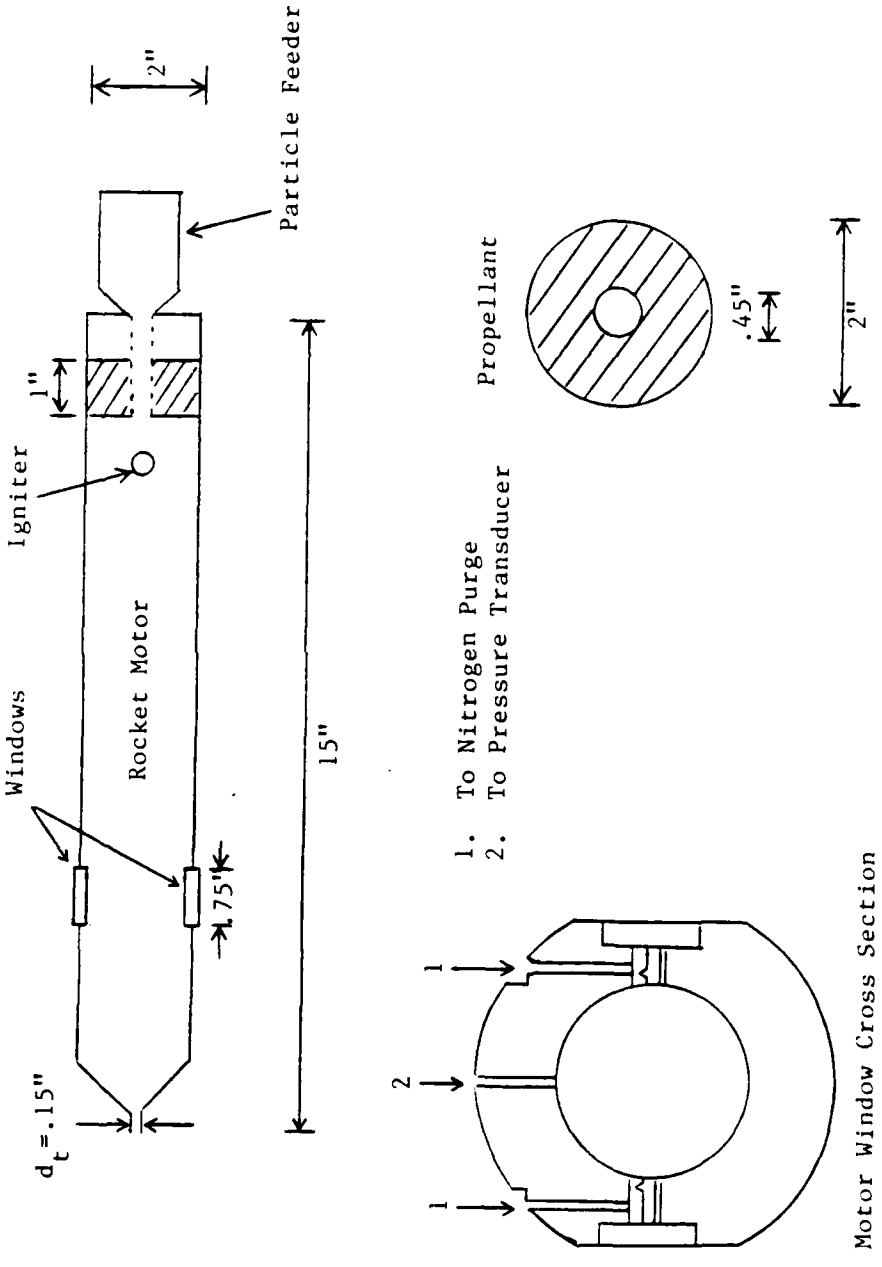


Figure 3.2 Schematic of Motor

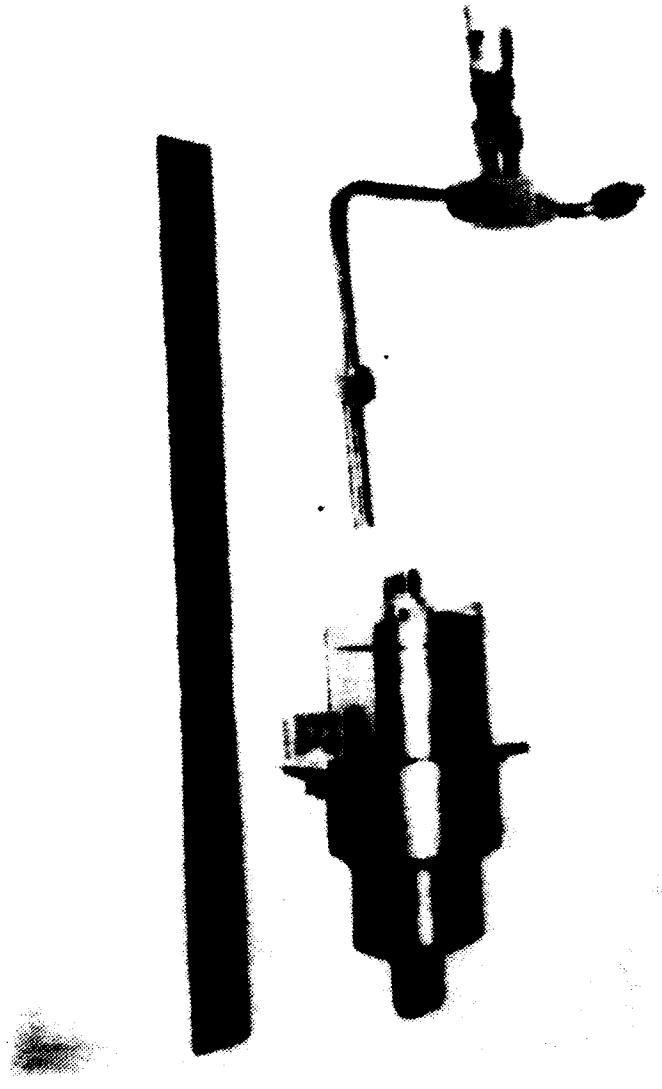

Figure 3.3 Photograph of Particle Feeder

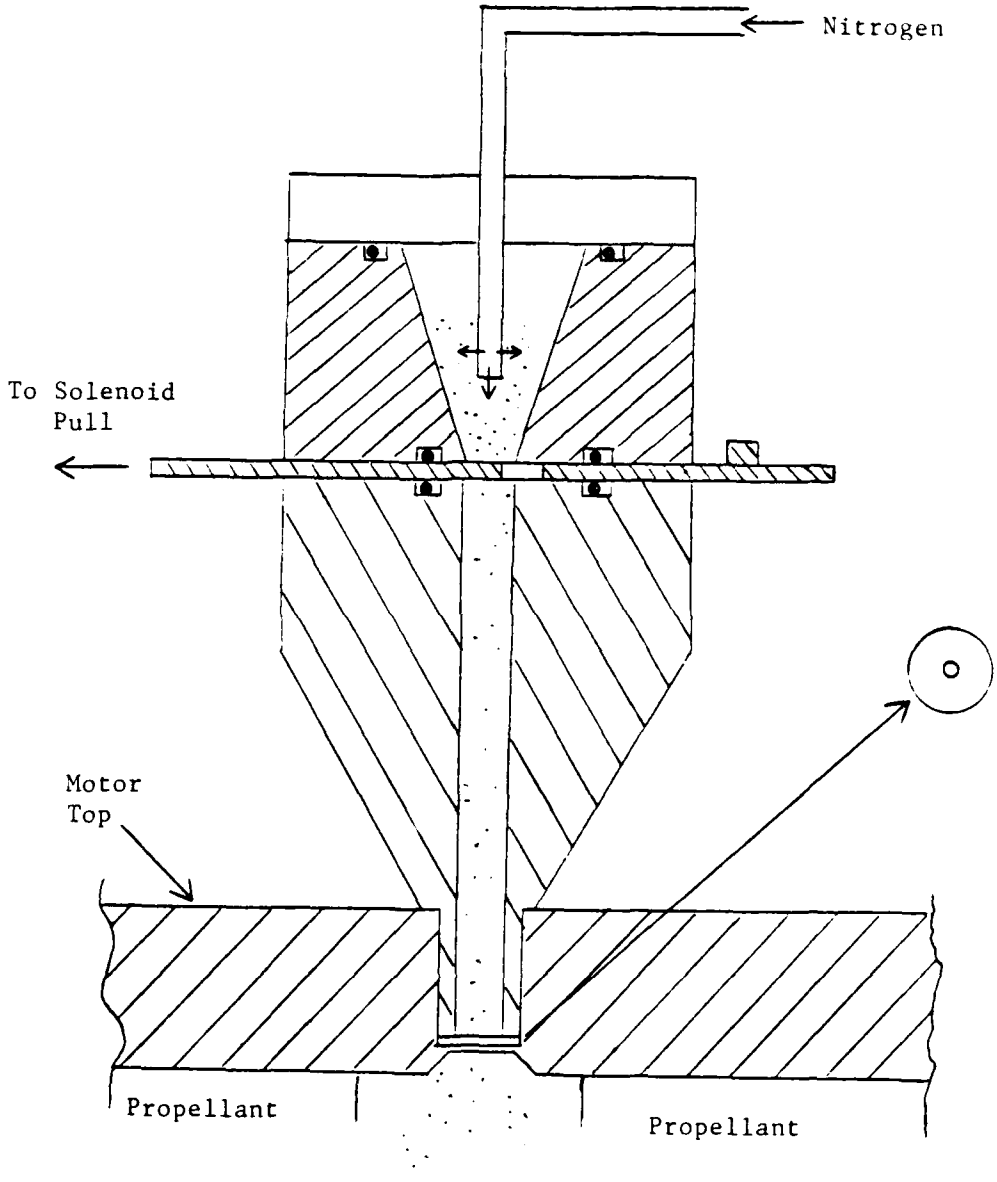


Figure 3.4 Schematic of Particle Feeder

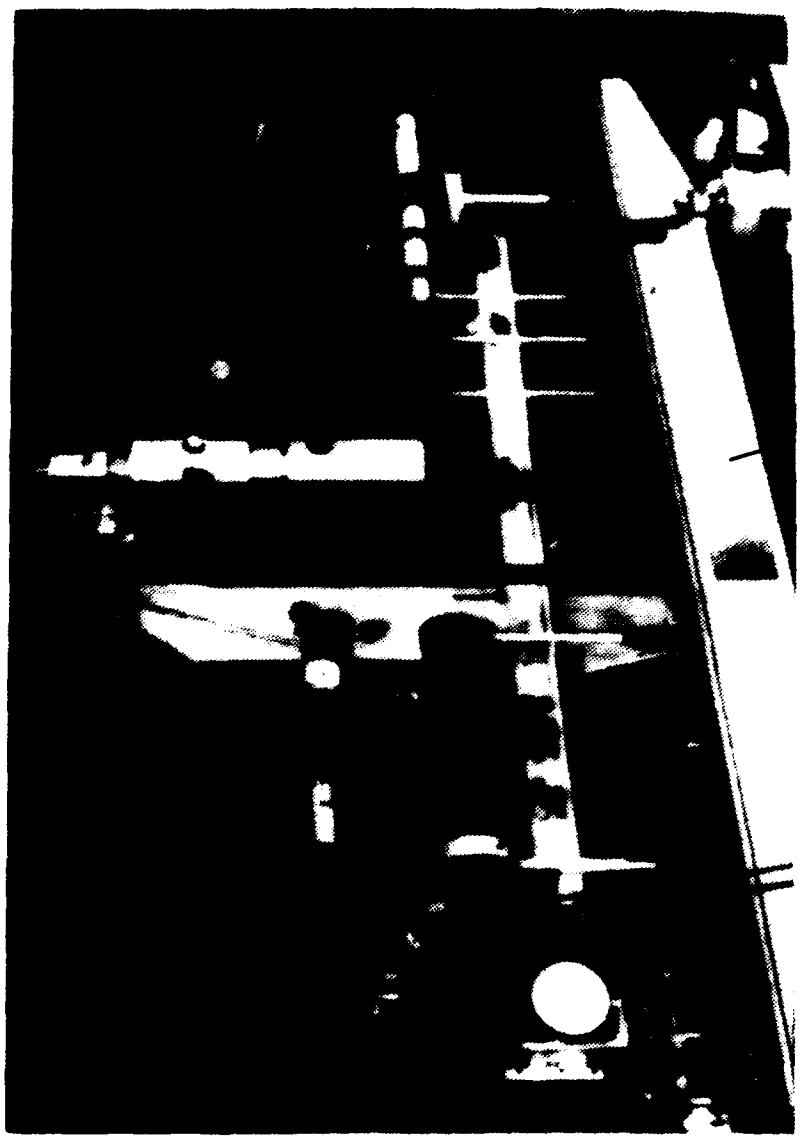

Figure 3.5 Photograph of Light Scattering Apparatus

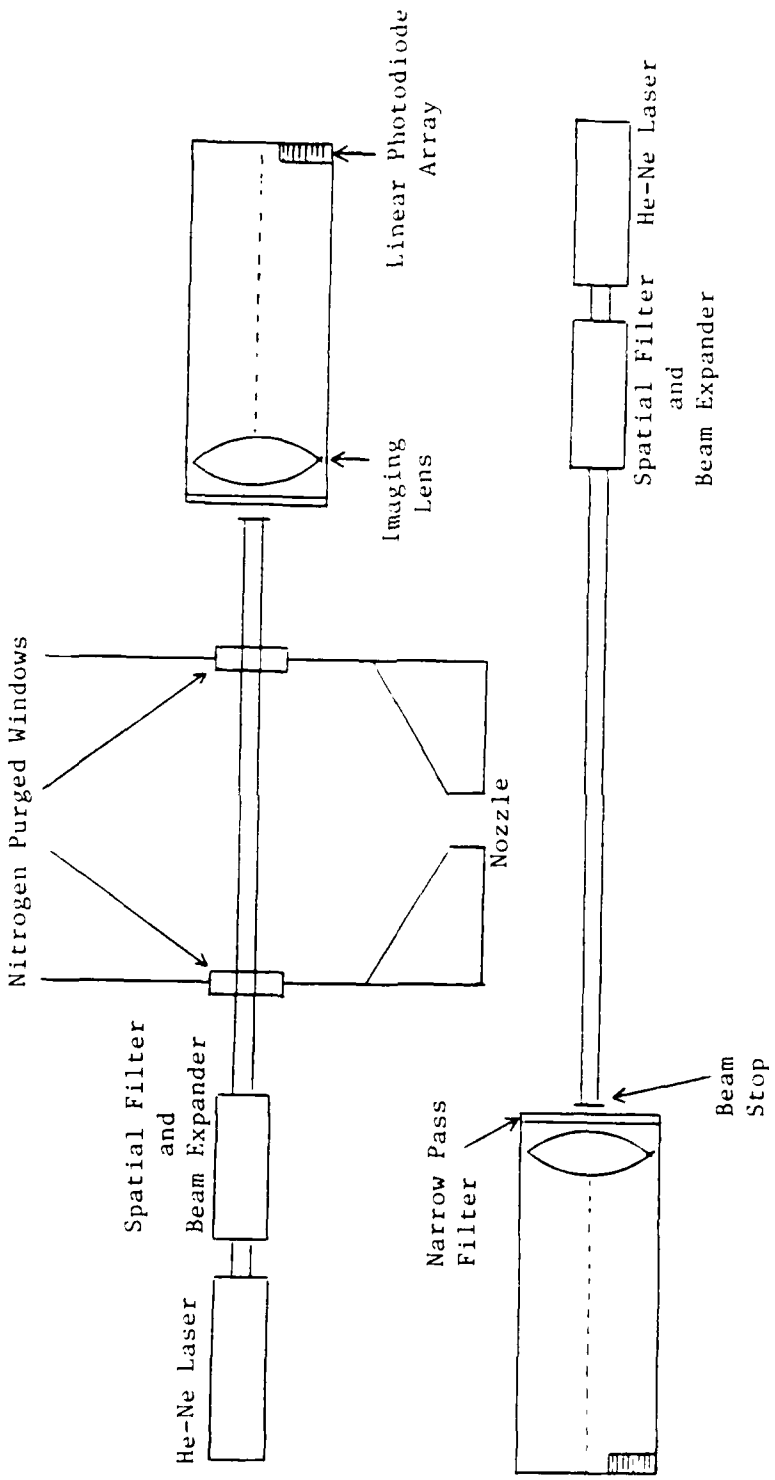


Figure 3.6 Schematic of Light Scattering Apparatus

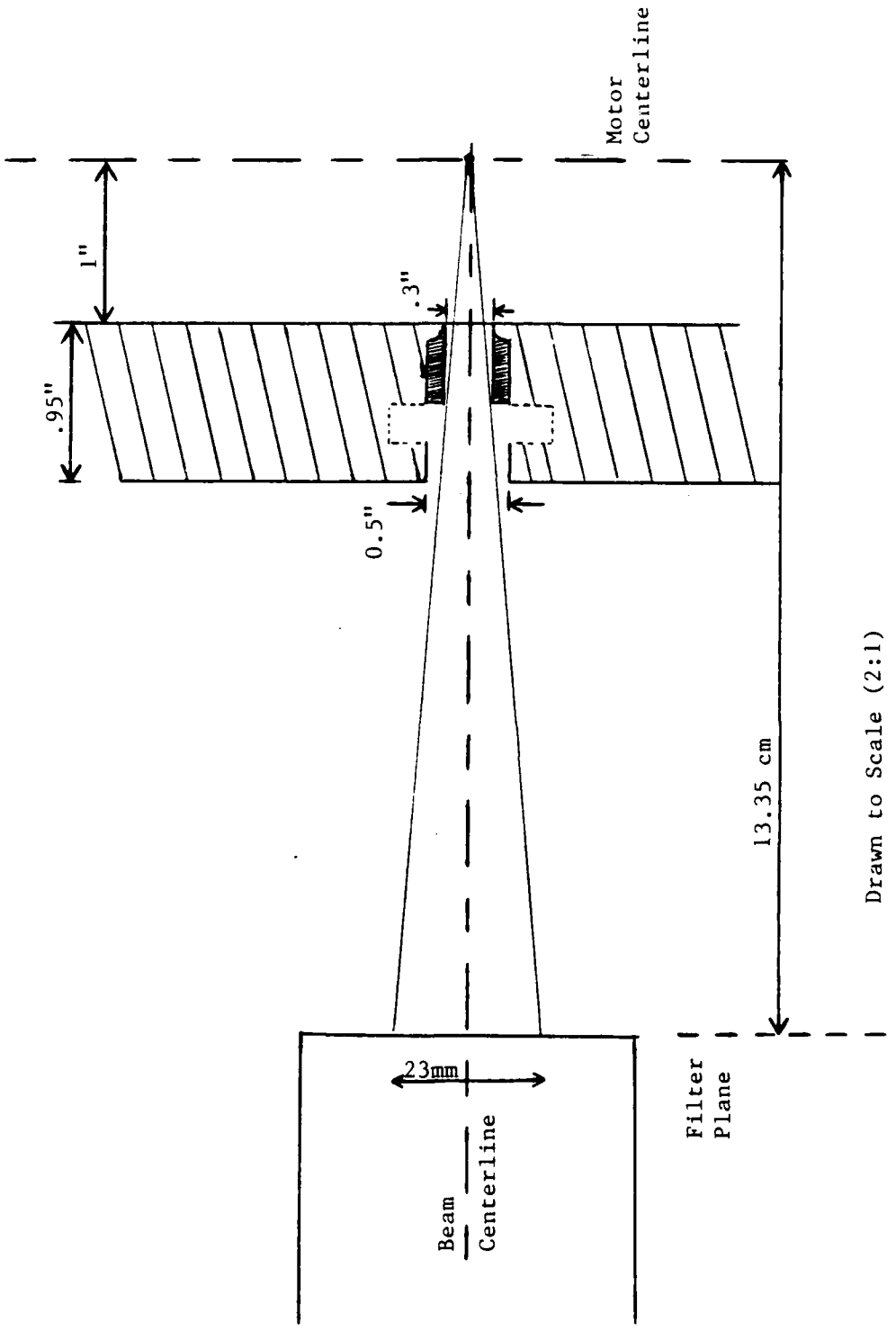


Figure 3.7 Motor Beam Pre-Lens Schematic

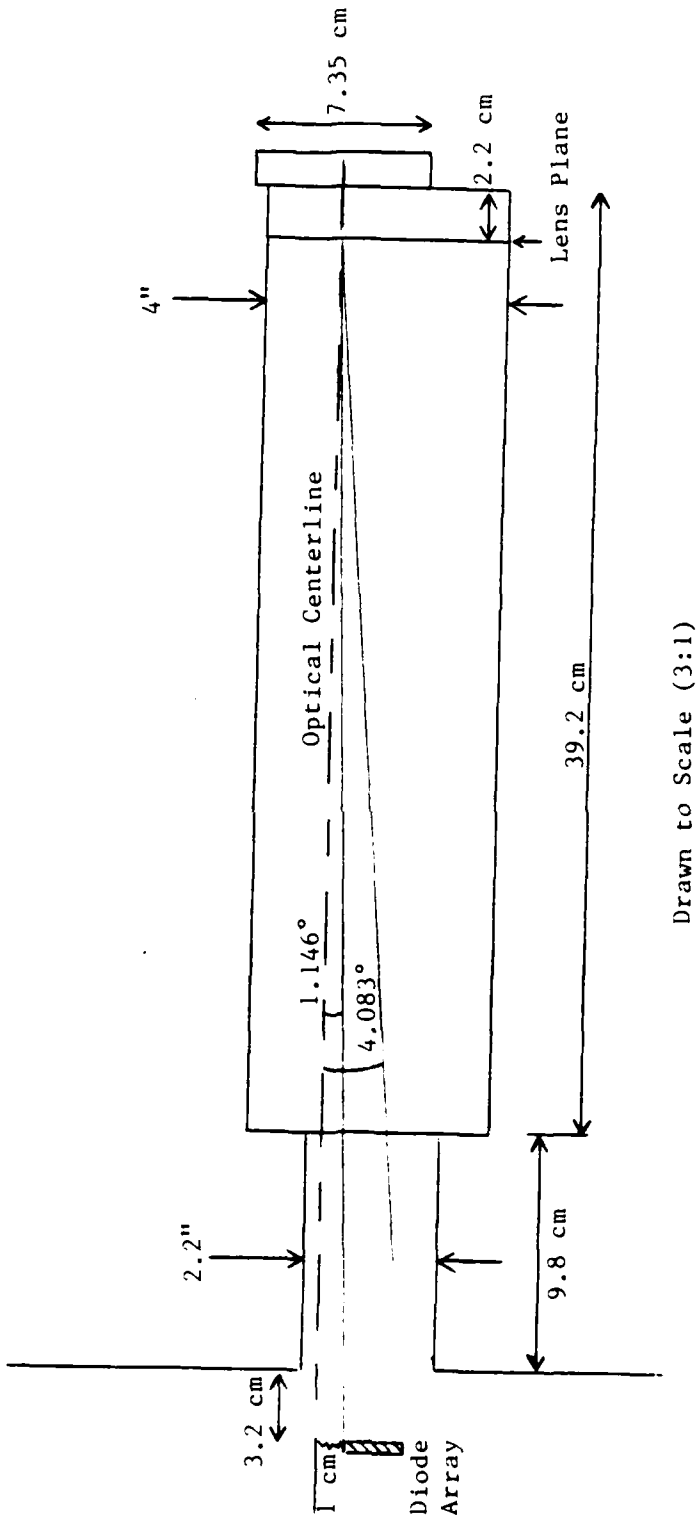


Figure 3.8 Motor Beam Post-Lens Schematic

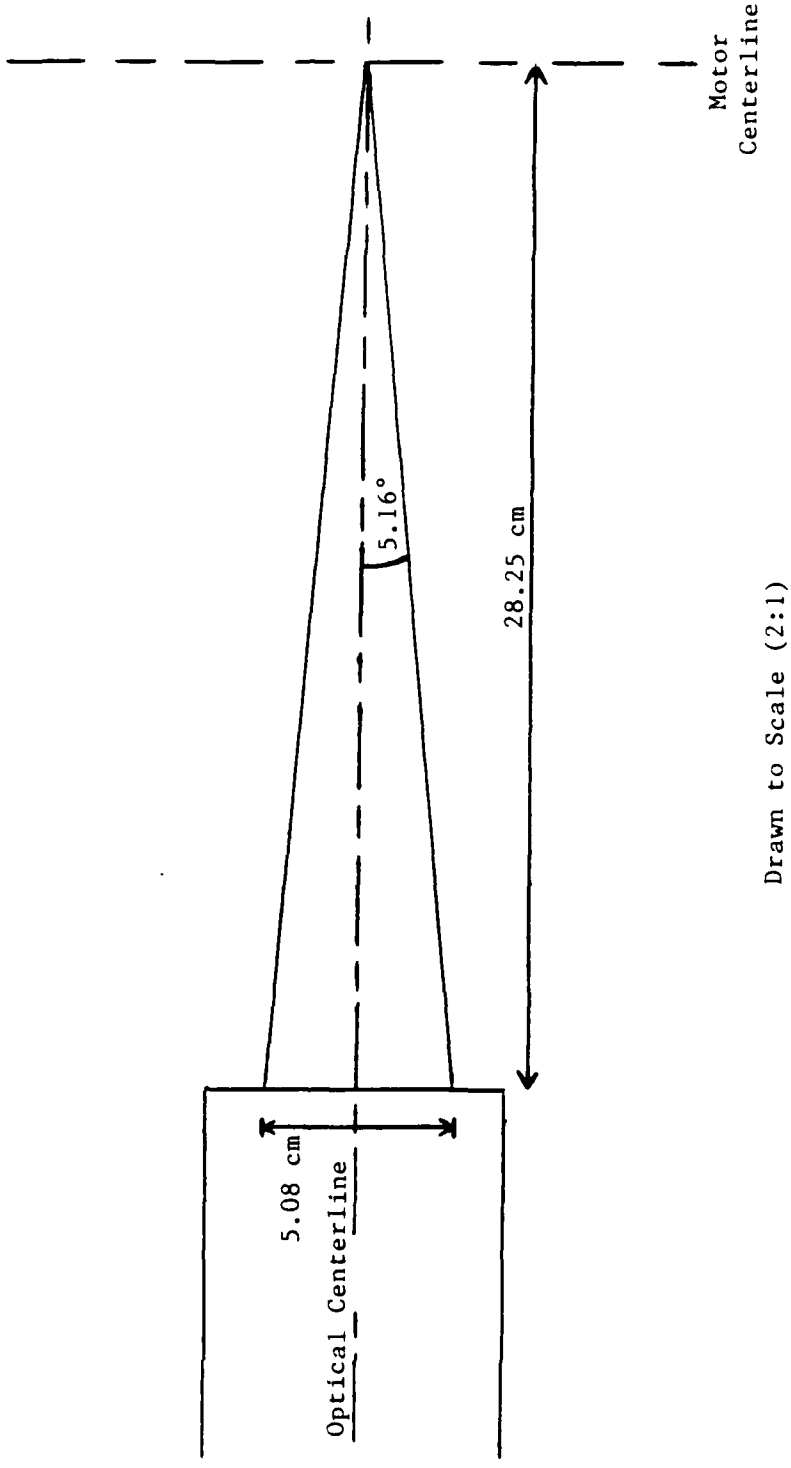


Figure 3.9 Exhaust Beam Pre-Lens Schematic

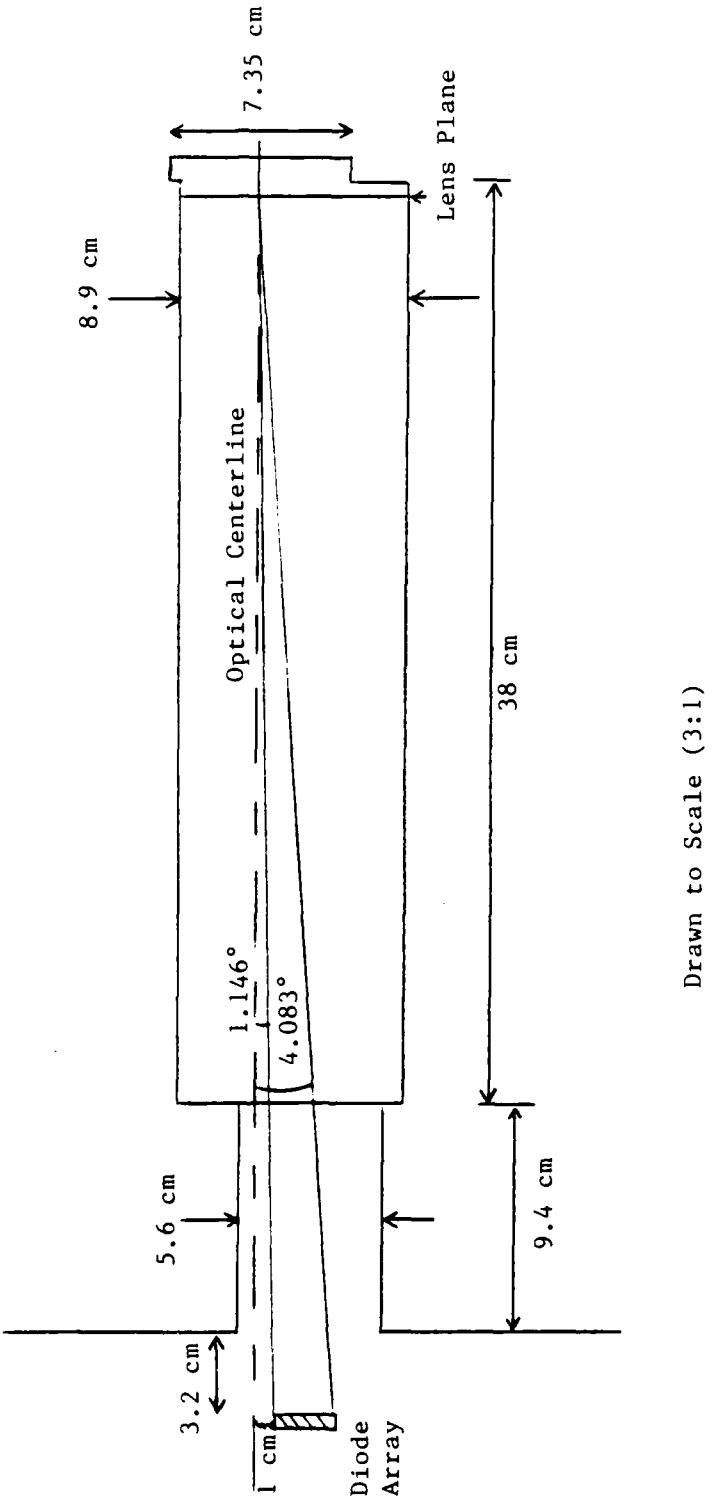


Figure 3.10 Exhaust Beam Post-Lens Schematic

TABLE I

NOZZLE SPECIFICATIONS

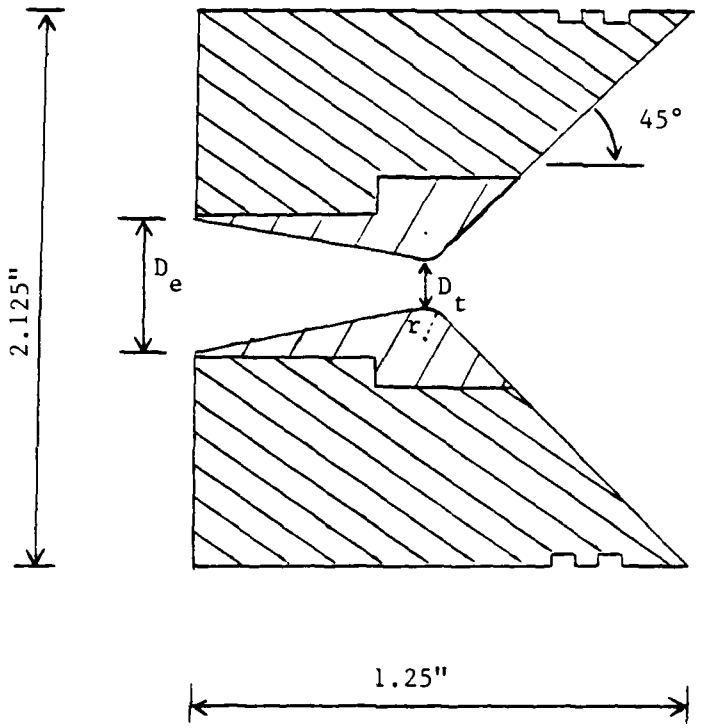


| Nozzle Type | Diameter Throat ($D_t$) (inches) | Diameter Exit ($D_e$) (inches) | Throat Radius (r) (inches) |
|---|---|---|---|
| Converging | .158 | .15 | None |
| Converging-Diverging | .154 | .277 | .075 |
| Converging-Diverging | .153 | .277 | .15 |
| Converging-Diverging | .345 | .427 | .20 |

TABLE II

LASER SPECIFICATIONS

| | | |
|---|---|---|
| A. | Helium-Neon Laser (Exhaust) | |
| | 1. Manufacturer | Spectra-Physics |
| | 2. Model: | 147 |
| | 3. Type: | He-Ne Class IIIB |
| | 4. Output Power: | 8 mWatt |
| | 5. Beam Diameter: | .92 mm |
| | 6. Beam Divergence: | .87 nrad. |
| B. | Helium-Neon Laser (Motor Cavity) | |
| | 1. Manufacturer: | Uni-Phase |
| | 2. Model: | 1305P |
| | 3. Type: | He-Ne Class IIIB |
| | 4. Output Power: | 5 mWatt |
| | 5. Beam Diameter: | .81 mm |
| | 6. Beam Divergence: | 1.00 mrad. |

# IV. RESULTS AND DISCUSSION

## A. SYSTEM CALIBRATION

The light scattering apparatus was calibrated to ensure that the system was accurately measuring particle size. The first half of the calibration consisted of beam spread tests in which the two light beams were checked for temperature and density gradient effects using a non-metallized propellant. The second half of the calibration involved using the scattering apparatus to measure the diameter of particles in solution. The particles were of known size and were used to judge system accuracy.

The intensity of a light beam will decrease and the beam will spread a small amount as it passes through a hot gas jet containing no particles. The purpose of these tests was to measure the severity of these effects in order to determine if particle scattering data would be effected. The beam spread test was conducted by placing neutral density filters in front of the photodiode array and then raising the array until the beam struck near the middle. A dummy firing run was conducted to record a baseline Gaussian trace after which an actual firing occurred and the beam profile was recorded once again. The two traces were then compared. The exhaust beam traces are shown in Figure 4.1. The temperature and density gradient effects in the exhaust were observed to be minor. The motor beam traces during

initial testing are depicted in Figure 4.2. The beam was not recorded on the diode array during the test. This result will be discussed in the section entitled Motor Laser Beam Problem.

Two particle sizes, 5.1 microns and 0.8 microns, were used in the second half of the calibration. The scattering apparatus was set with the photodiode arrays lowered one centimeter below the optical centerline. This measured the scattering angles between 1 and 4 degrees as per Figure 3.10. The 5.1 micron particles were suspended in a solution of distilled water and the light scattering profiles in both beam paths were recorded (Figure 4.3 and 4.4). The $D_{32}$ was measured to be 5.1 microns through the motor and 5.4 microns for the exhaust beam, in excellent agreement with the particle manufacturer's data. Following this, a solution of 0.8 micron particles was measured using the same procedures. The results, Figures 4.5 and 4.6, showed no correlation and demonstrated the problem of trying to measure particles less than approximately 3 microns using the present optical components and positions. The 5.1 micron particles diffracted light such that 46% of the scattered light in the forward lobe was measured by the system. The 0.8 micron particles diffracted light at larger angles, such that only 9% of the light scattered in the forward lobe was measured by the system (see Figure 4.7). This means that the concentration of small particles, less than approximately 3 microns, must be very high in order to develop enough scattered light to be measured.

The final phase of the calibration tested the system's response to a bimodal distribution which would be typical in the solid propellant rocket motor exhaust. The 5 micron particles were mixed with the 0.8 micron particles in a ratio of roughly 1:25. In both beams, Figures 4.8 and 4.9, the $D_{32}$ came out to be essentially the diameter of the large particles. The larger particles scattered much more measurable light and dominated the scattering profile, even though there were far fewer large particles in the mixture. Of course, $D_{32}$ is also dominated by the larger particles in the distribution.

The calibration was successful in determining particle sizes larger than 5 microns. Difficulty could be expected in trying to measure particles smaller than three microns. The calibration reconfirmed that $D_{32}$ is heavily weighted towards measurement of large particles in a polydispersion.

## B. MOTOR LASER BEAM PROBLEM

The motor optical bench presented its own unique characteristics which made motor beam alignment an important consideration. They were: (1) the motor beam had to travel through the center of both windows without refraction, (2) slight angular displacements were magnified as the light passed through the motor windows, (3) the windows caused undesirable multiple reflections, (4) the cantilever arrangement of the motor optical bench was very sensitive to vibrations.

The motor laser system was carefully aligned. After alignment, motor firings for particle measurement were conducted using the X-55 propellant. These firings typically reached a peak pressure of 300 psi with no steady state chamber pressure. Particle injection consistently indicated approximately 20 micron particles in the motor. This was true even when the particle feeder became clogged with moisture and particle fall was questionable. Several firings were made without particle injection. These results are depicted in Figures 4.10 and 4.11. These graphs display the 20 micron slope, diode saturation at the smaller angles, and an unsteady behavior which included some "zero" traces. The "zero" traces indicated that on some of the scans of the diode array no scattered light was received, as expected with no particles present. This contrasted sharply with other traces during the same run in which the diode array was saturated with maximum voltage toward the upper portion of the array.

A check was made of the X-55 propellant to see if there might be particulate matter in the propellant which could result in this behavior. Scanning electron microscope photographs were taken (Figure 4.12) but the results were inconclusive. A small number of 20 micron particles were found. Their composition was unknown, but it seemed unlikely that the small number of 20 micron particles found could be responsible for the motor laser problem.

The next check made was to determine if the rocket combustion was generating any light at .6328 microns. Firing the motor with the laser off produced no light on the diode array indicating there was no combustion light at .6328 microns.

The vibration sensitivity of the motor laser was then suspected. The various components of the system were tapped and vibrated while watching the diode trace on an oscilloscope, but the trace remained relatively steady even under some heavy tapping.

Other possible sources for the motor laser beam problem were window movement under pressure, nitrogen purge (for the windows), and motor temperature gradient effects. Window movement was checked by capping the nozzle and pressurizing the motor to 250 psi. This had a negligible effect on the diode trace. The nitrogen purge for the windows had no effect on the trace when used without a motor firing. Density gradients created during a firing, however, could be a problem. Finally, a torch was placed in the motor to study temperature effects. The nitrogen purge was turned on and off to look at the effects of the interaction of the hot and cool gases. In all cases the temperature gradients caused only a minor fluctuation in the diode trace.

The beam spread tests conducted during calibration were of particular importance. The motor beam Gaussian disappeared completely from the diode array during the motor firing. A

large (0.5 inch diameter) active area photodiode was used to measure transmittance and showed that approximately 60% of the light was transmitted through the test section.

Attempts to stabilize the beam were initiated with the use of a spatial filter and collimating lens. It proved to be extremely difficult to place a spatial filter and a collimating lens in the beam path prior to the test section. Their use resulted in small angular displacements from one optical piece to the next, which were magnified through the test section. This problem was overcome by building a one-piece spatial filter and collimating lens. The lens was affixed to the front of the spatial filter. This arrangement proved to be very effective in stabilizing the beam. An added benefit from the filter and lens was the doubling of the diameter of the beam to 0.1 inches. If beam alignment with the diode array was a problem, then a broader beam would help alleviate it. A subsequent beam spread test produced the surprising result that the motor beam still disappeared from the diode array during motor firing.

The next test performed on the system was a cold flow check. High pressure nitrogen was injected into the top of the motor and allowed to flow out the nozzle, simulating an actual firing. The pressure was brought rapidly up to 300 psi. During the test the diode trace on the oscilloscope disappeared while the pressure was building in the motor. While the pressure was a constant 300 psi the trace returned

to normal. When the pressure returned rapidly to zero the trace disappeared again. The source of the problem had finally been identified. Transient pressure gradients in the motor during pressure rise were causing the beam to bend downward. Transient pressure gradients in the motor during pressure fall-off were causing the beam to bend upward. This phenomenon explained both the beam disappearance from the diode array in the beam spread test and the random, high intensity signals recorded at larger scattering angles. The beam disappeared from the diode in the beam spread test because the motor data was taken during the pressure rise in the motor and, therefore, the beam displaced down and off the diode array (Figure 4.13).

In a similar fashion, the scattered light measurement problem was caused by the beam being bent below the beam stop. The high intensity light then saturated the top of the diode. The 20 micron slope (Figure 4.11) was just the tail-off of the laser Gaussian on the array. The unsteadiness of the traces was probably caused by small pressure fluctuations. The zero traces that occurred during some of the runs resulted when the beam had risen back above the edge of the beam stop.

The beam spread test was performed again to test the transient pressure gradient hypothesis. The decision was made to attempt a neutral burn, during which the chamber pressure would be constant. The throat diameter of the nozzle

was increased to 0.25 inches to drop the pressure to approximately 50 psi, which would yield a 5-second neutral burn. The beam stop was moved to its lowest possible position. The motor traces from this test are recorded in Figures 4.14 and 4.15. The position of the Gaussian did not shift, however, there was significant attenuation (98%). This attenuation may have been caused by the presence of smoke in the combustion chamber. The possibility also exists that the attenuation could still be caused by the beam moving off the array due to pressure and/or thermal gradients. The use of ring diode arrays would significantly reduce this problem.

## C. MOTOR FIRING DATA

### 1. Metallized Propellant

Metallized propellant was fired in the motor at low pressure, 50 psi, in order to take data during the plateau portion of the burn. Attempts to modify the data acquisition system to take data at low pressure proved to be difficult. The $BKNO_3$ igniter introduced a pressure spike which sometimes caused the data to be taken before the propellant began to burn. To overcome this problem, data acquisition was initiated manually by throwing a switch when the pressure in the motor was heard. This generally resulted in the data being taken too late in the run.

Insufficient time remained to resolve all the difficulties, but the procedure of taking data during the plateau portion of the burn may be a partial solution to the motor laser beam problem.

2. Particle Injection

The nitrogen activated particle injection system was built and tested. In nonburning tests the injection system produced a steady mist of 15 micron aluminum particles through the combustion chamber for a period of approximately 6 seconds. During an actual firing at low pressure the particles again successfully passed from the hopper through the motor. The nitrogen particle injection system showed promise of being able to solve the earlier problem of combustion moisture clogging the particle feeder.

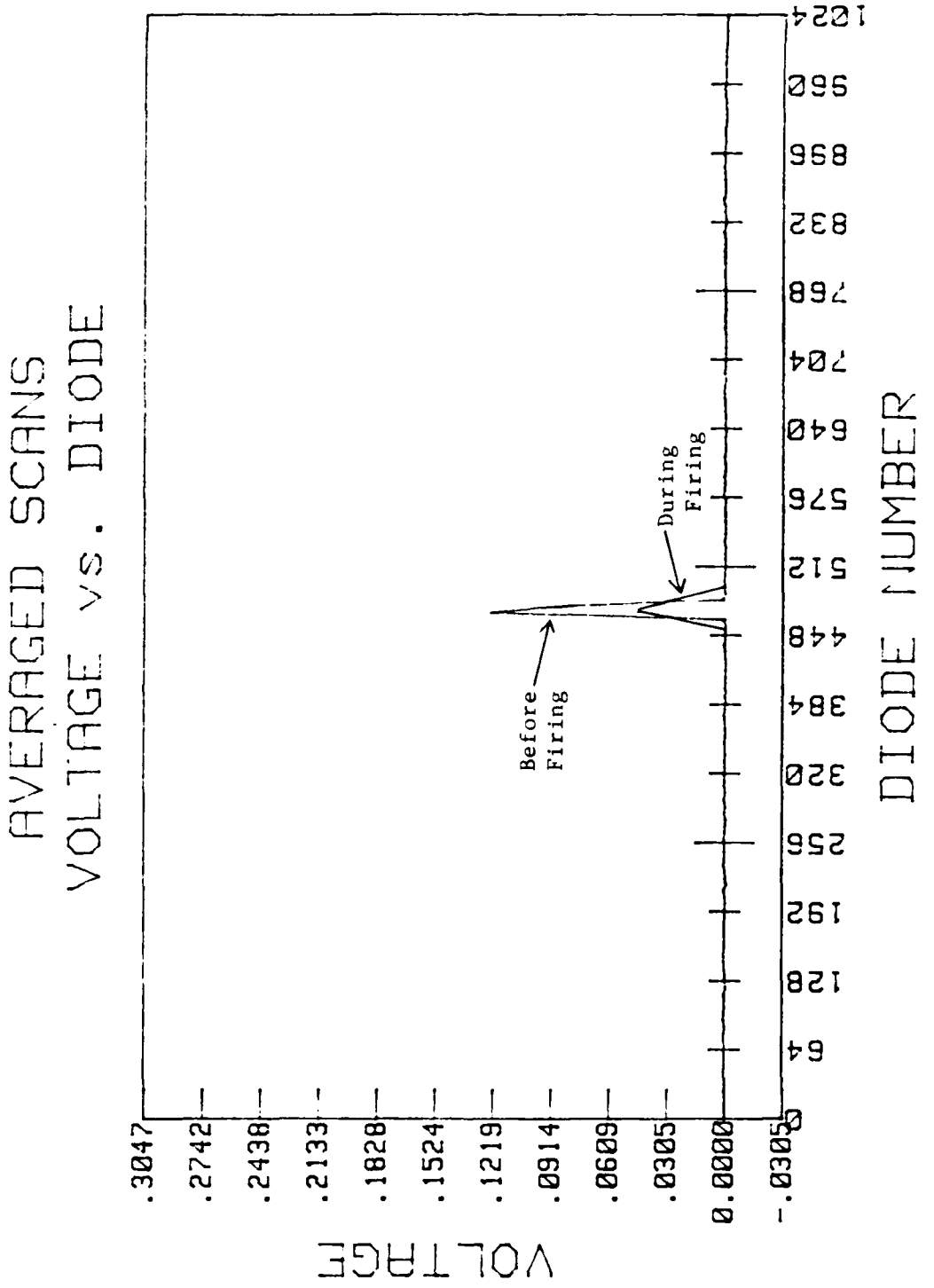


Figure 4.1 Exhaust Beam Spread Test

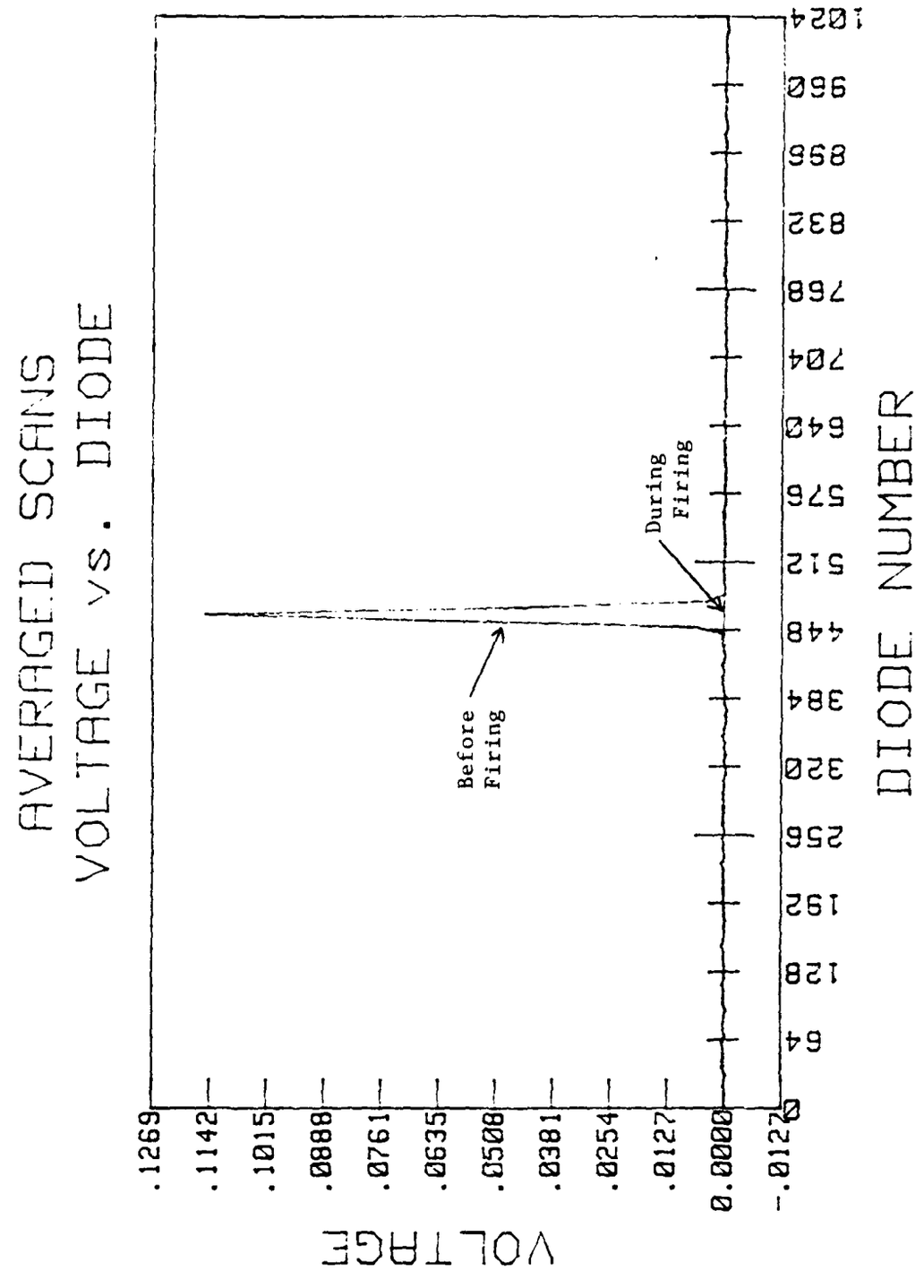


Figure 4.2 Motor Beam Spread Test

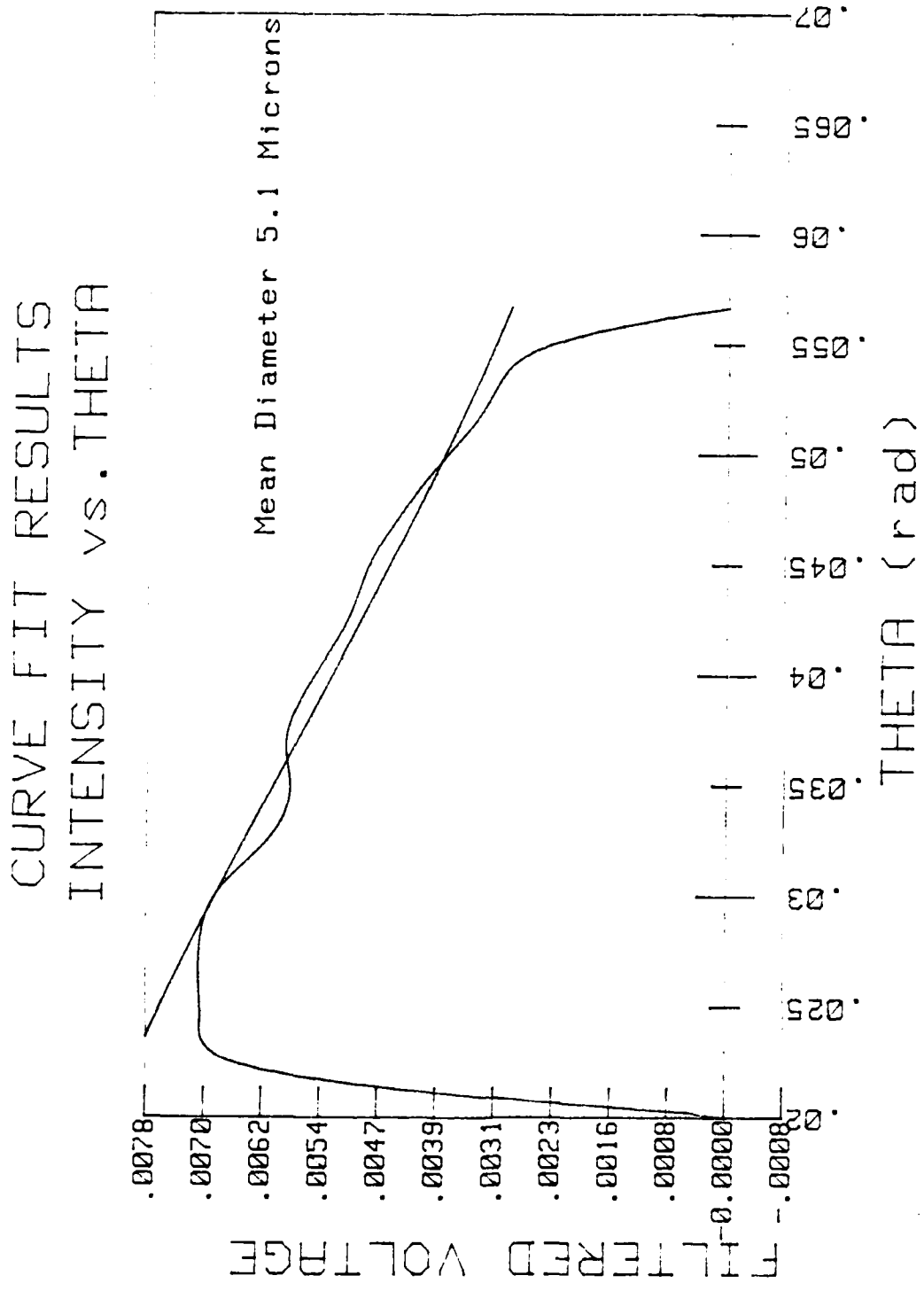


Figure 4.3 Motor Calibration with 5.1 Micron Spheres

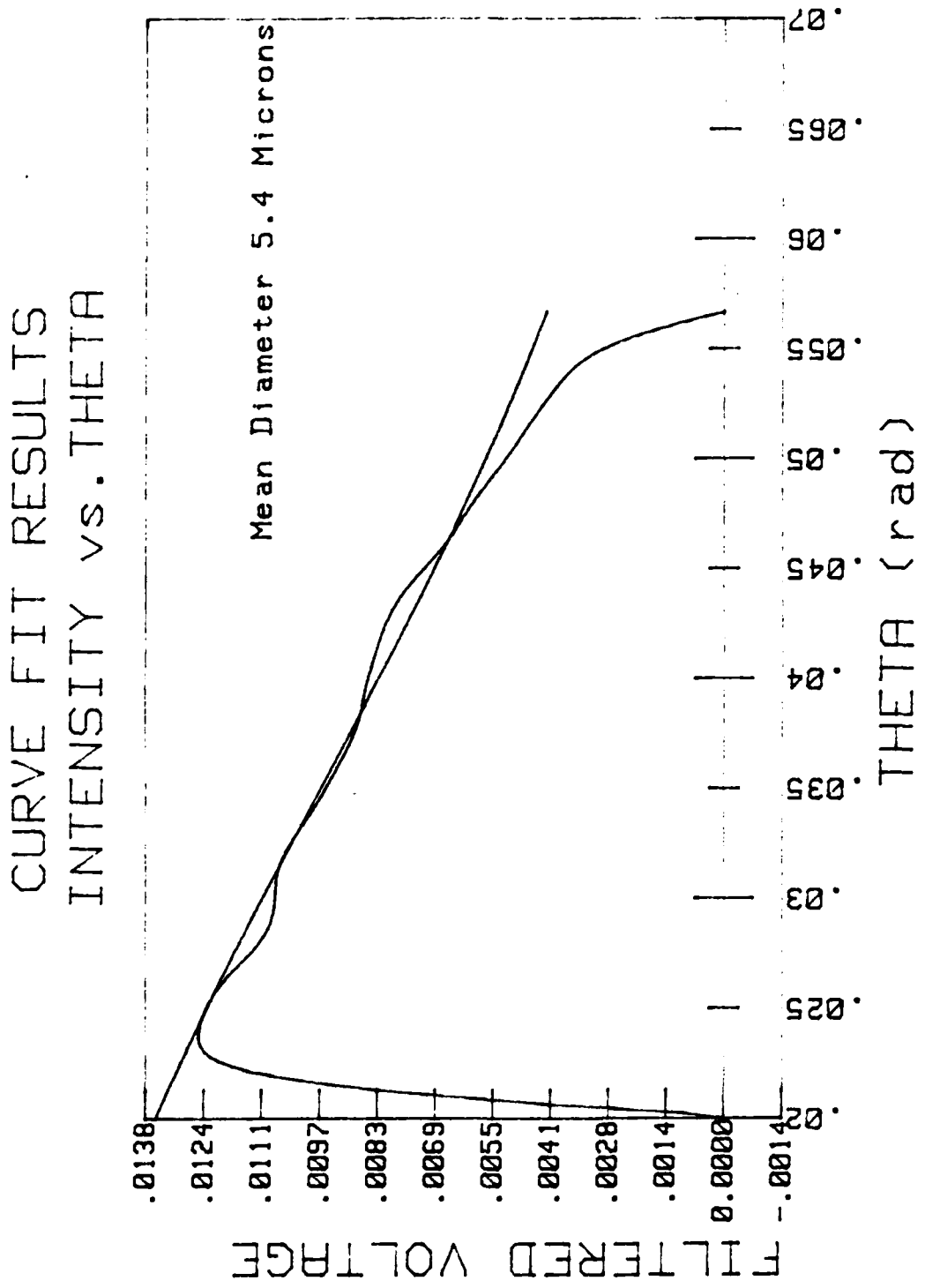


Figure 4.4 Exhaust Calibration with 5.1 Micron Spheres

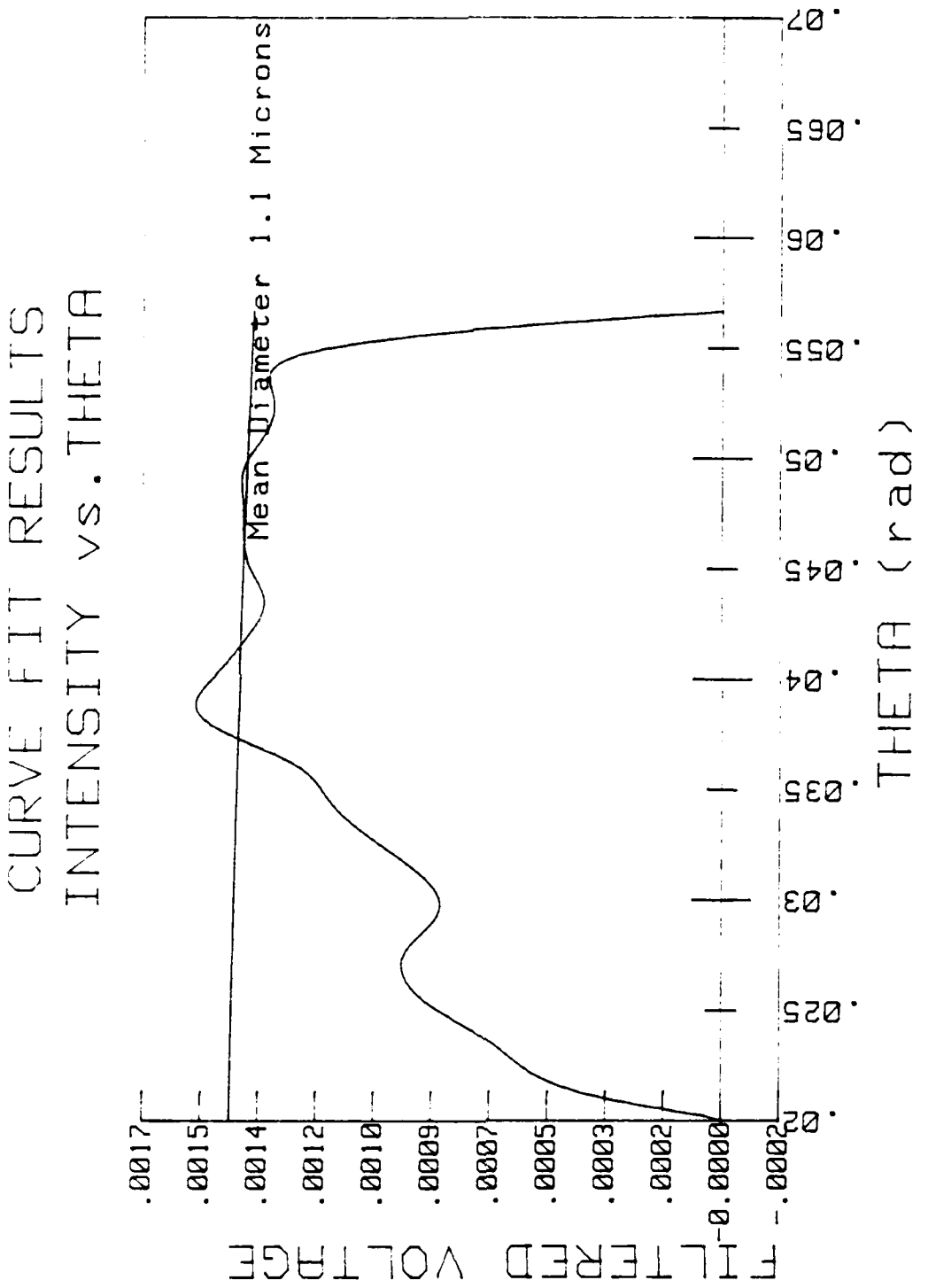


Figure 4.5 Motor Calibration with 0.8 Micron Spheres

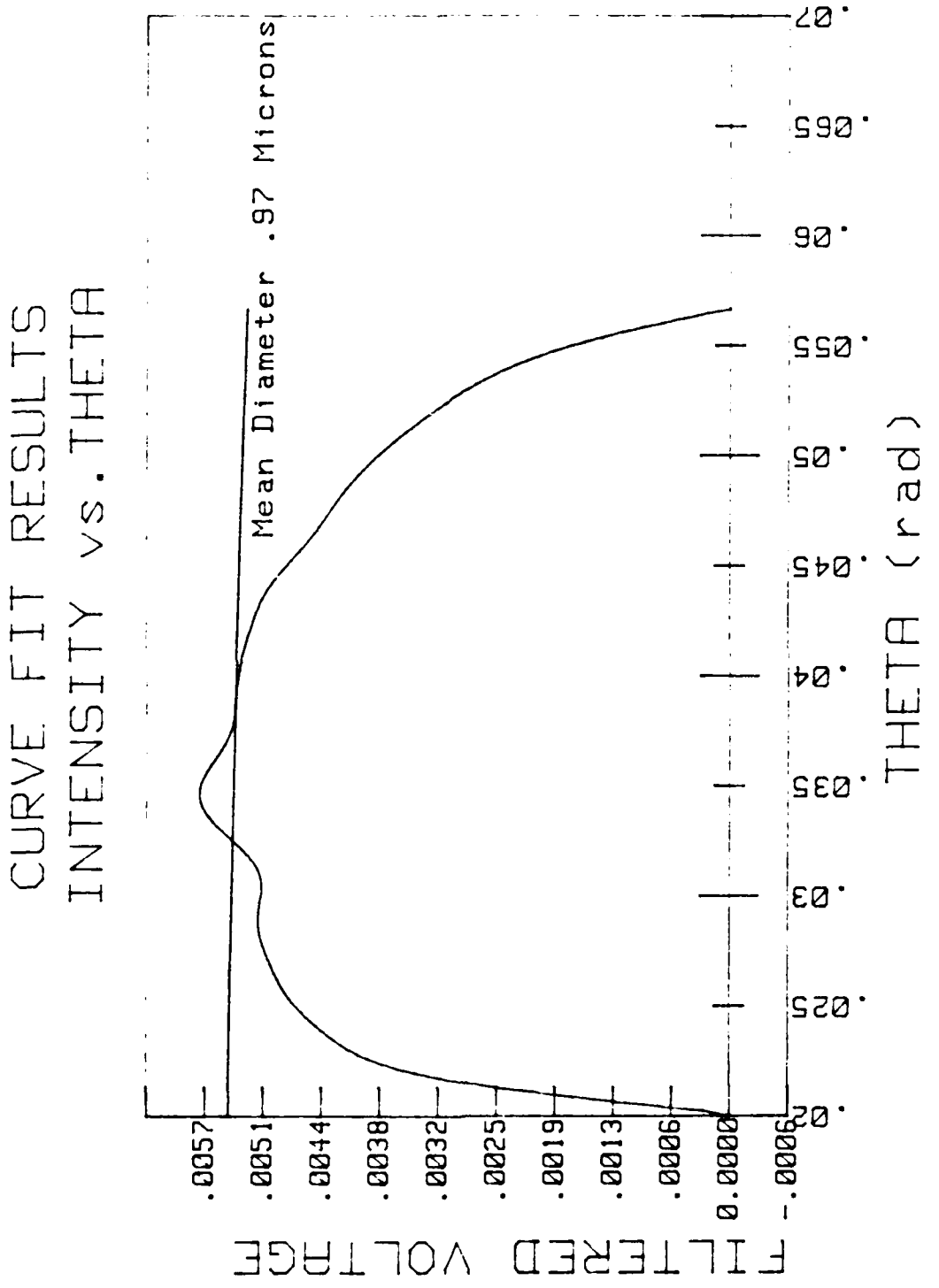


Figure 4.6 Exhaust Calibration with 0.8 Micron Spheres

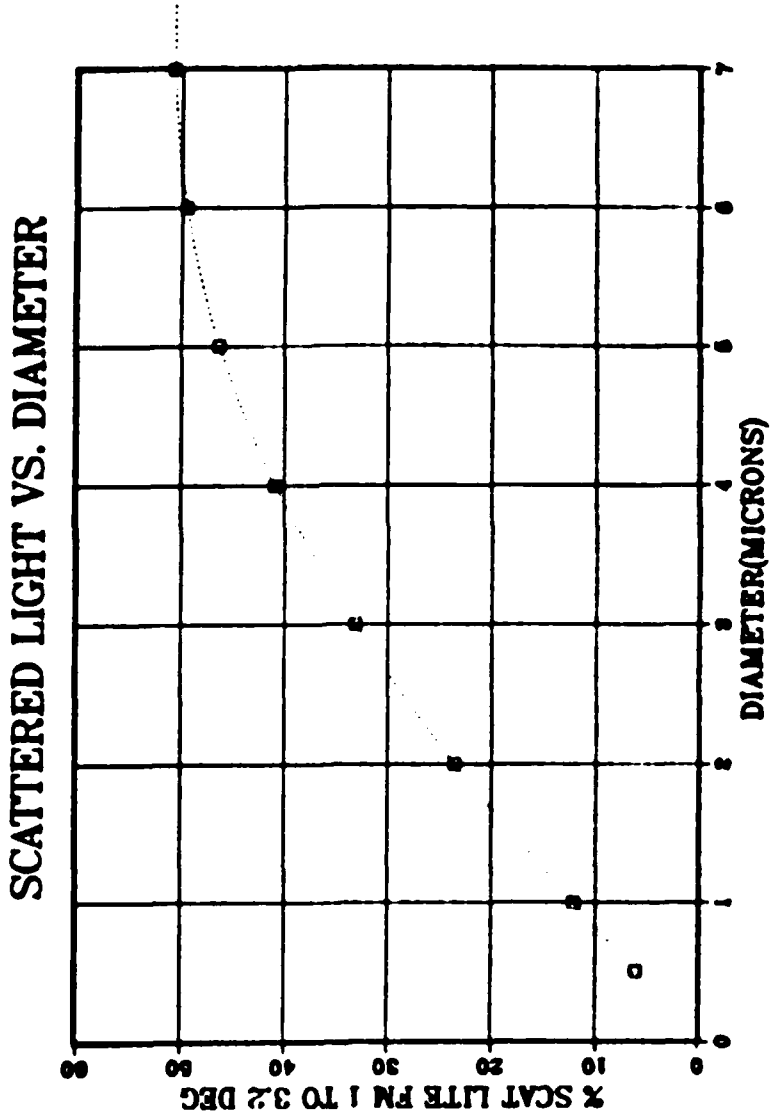


Figure 4.7 Graph of Scattered Light vs. Particle Diameter

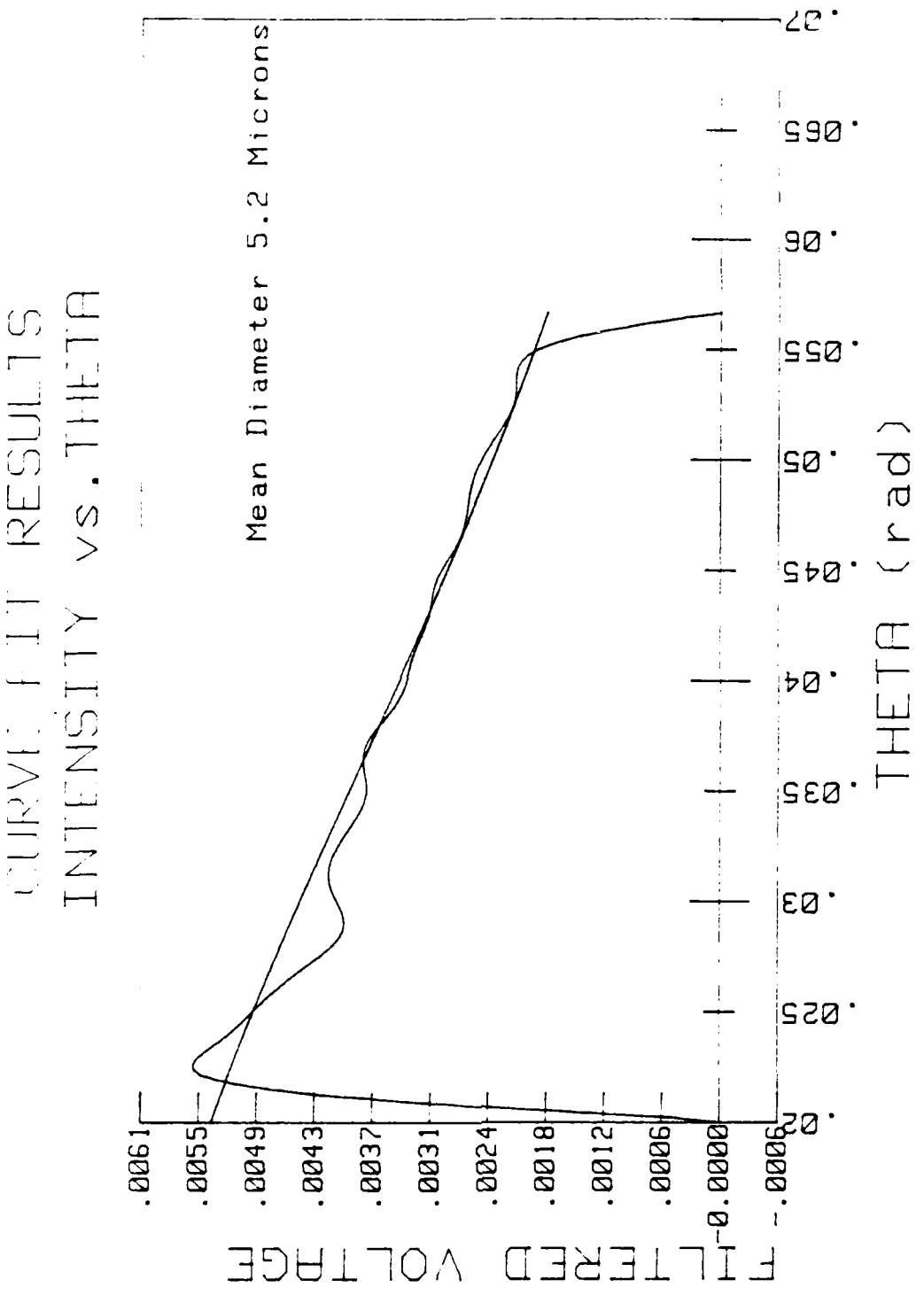


Figure 4.8 Motor Calibration with Bimodal Distribution

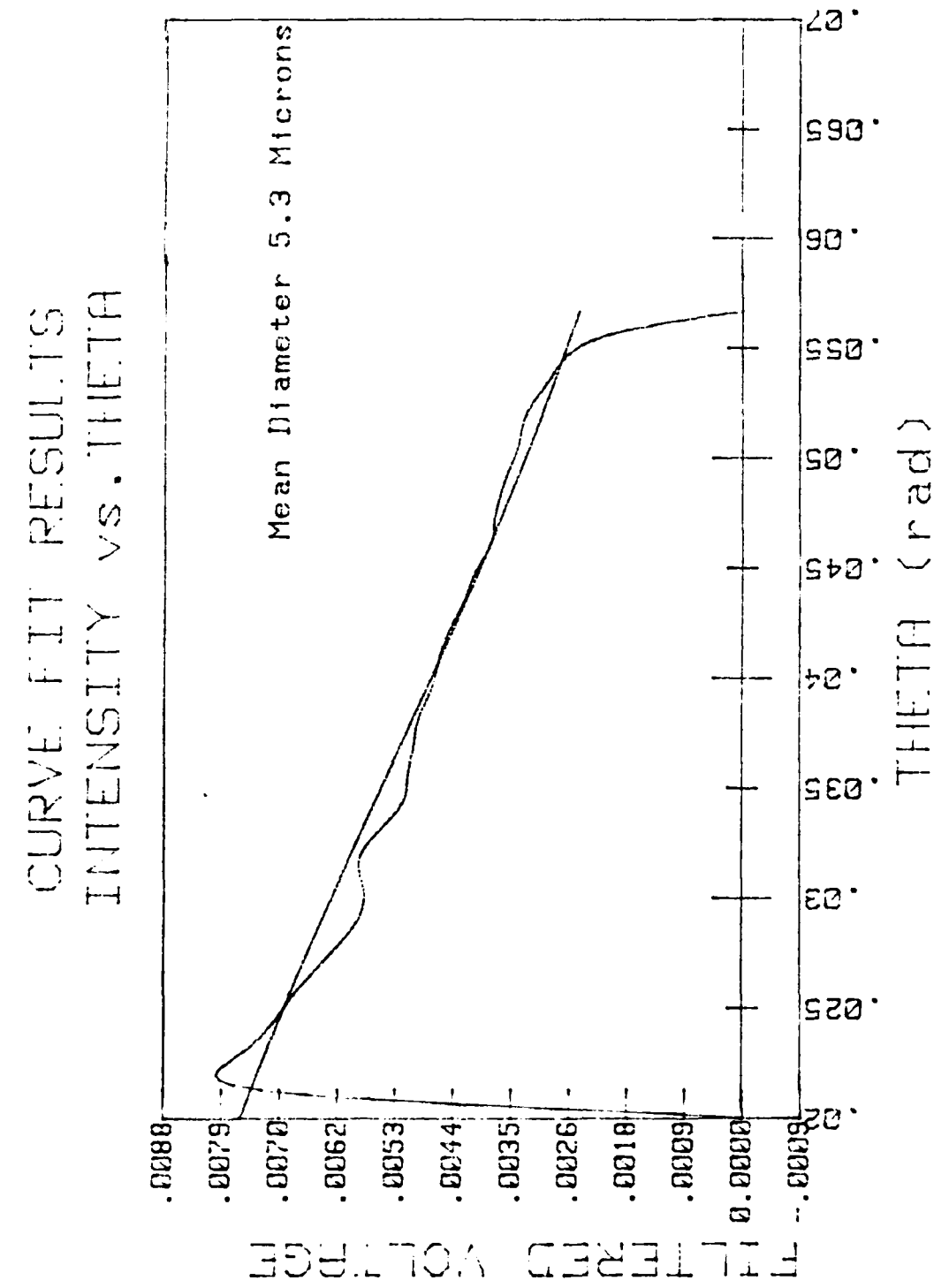


Figure 4.9 Exhaust Calibration with Bimodal Distribution

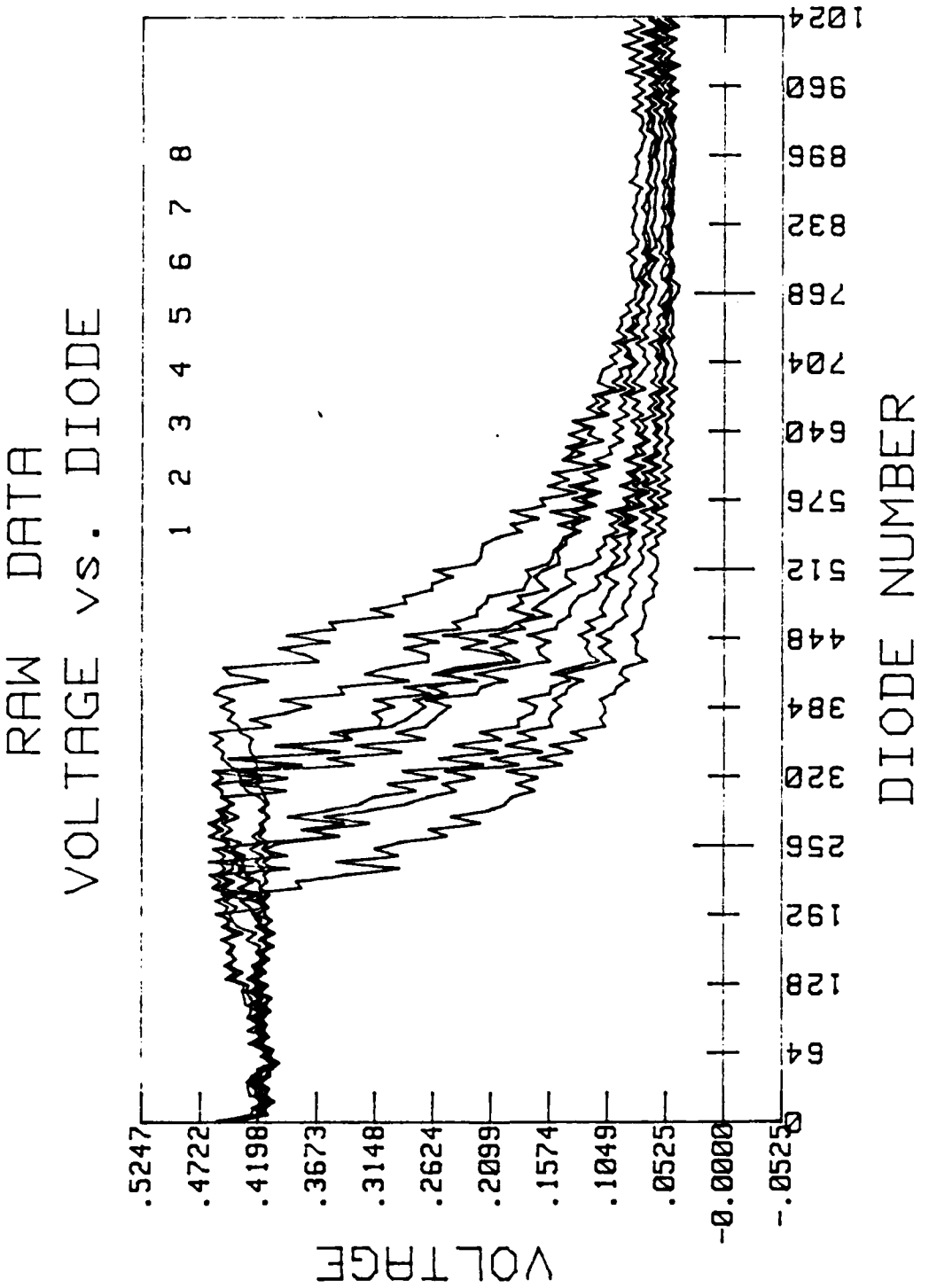


Figure 4.10 Motor Laser Traces without Particle Injection

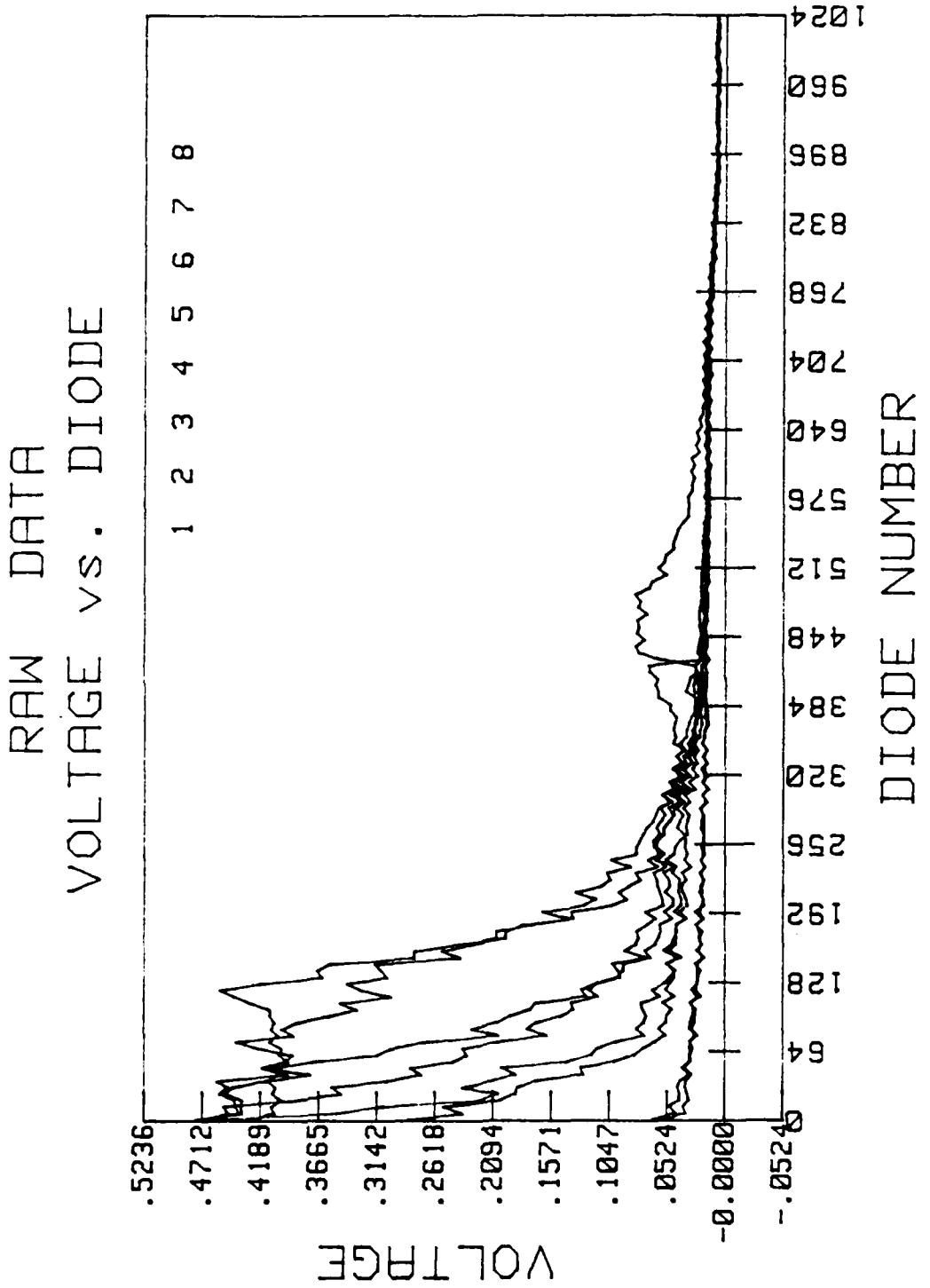


Figure 4.11 Motor Laser Traces without Particle Injection

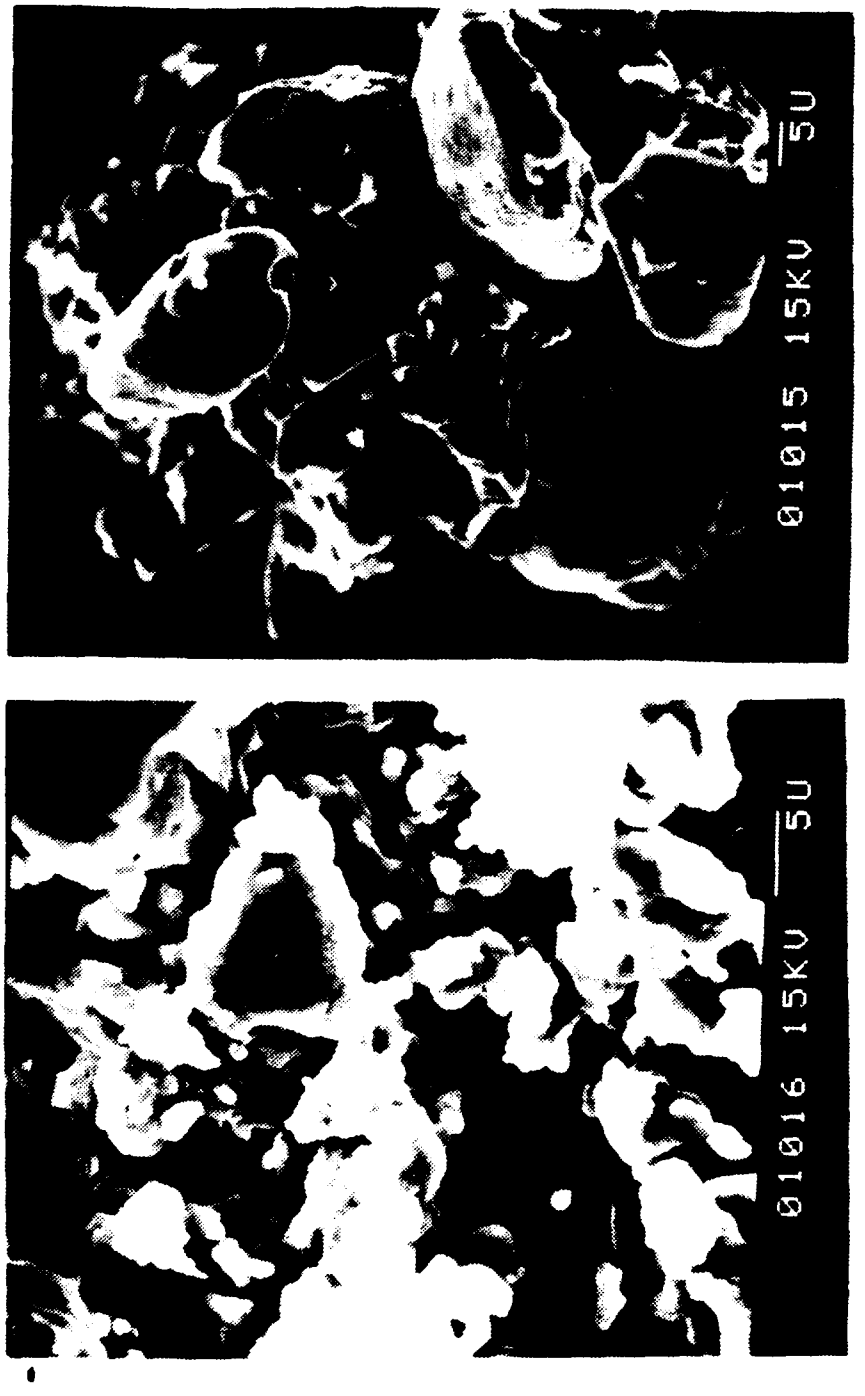


Figure 4.12 SEM Photographs of X-55 Propellant

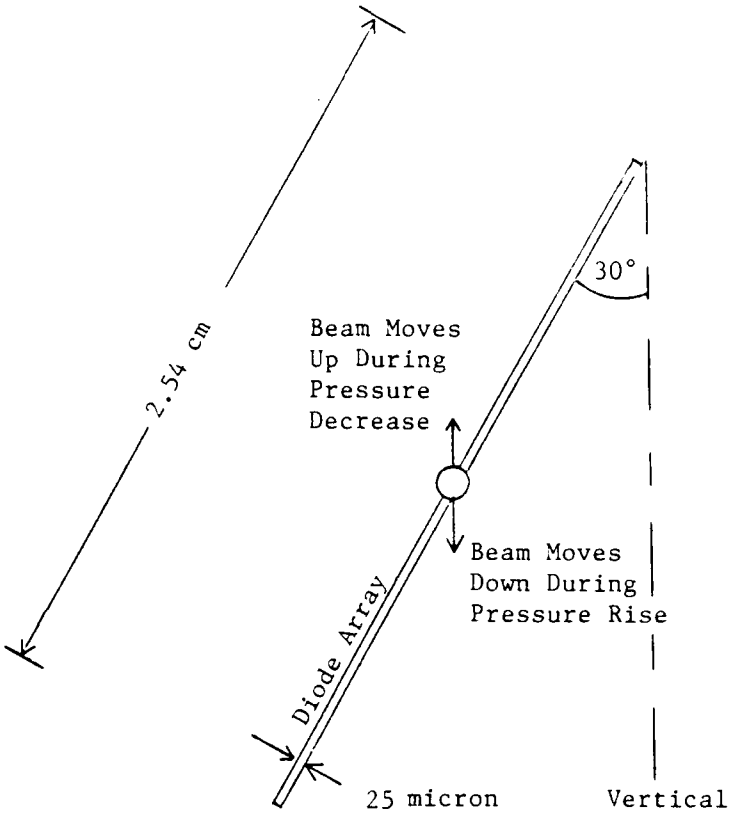


Figure 4.13 Motor Beam Transient Pressure Gradient Effect during Beam Spread Test

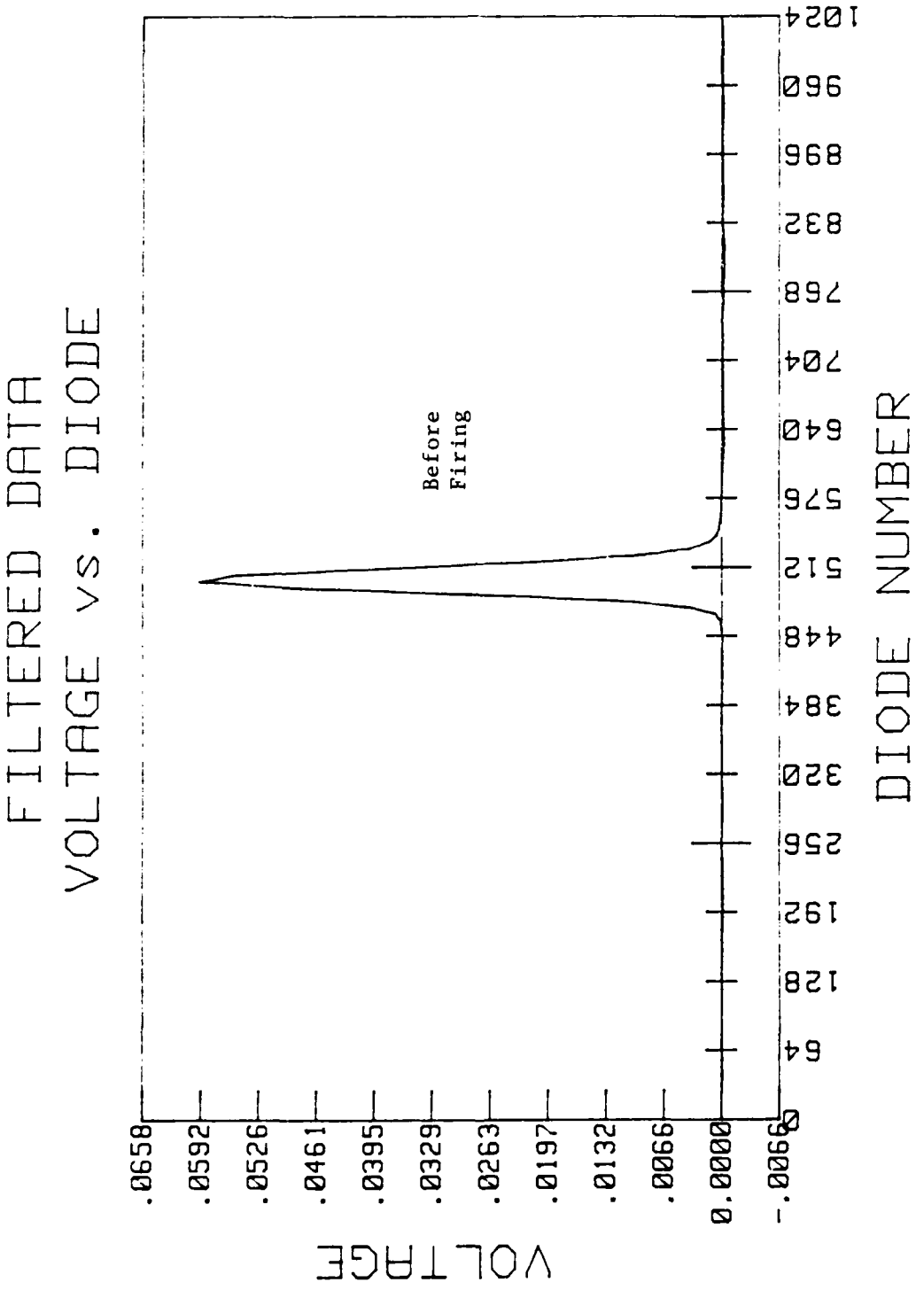


Figure 4.14 Motor Beam Spread Test at Low Pressure

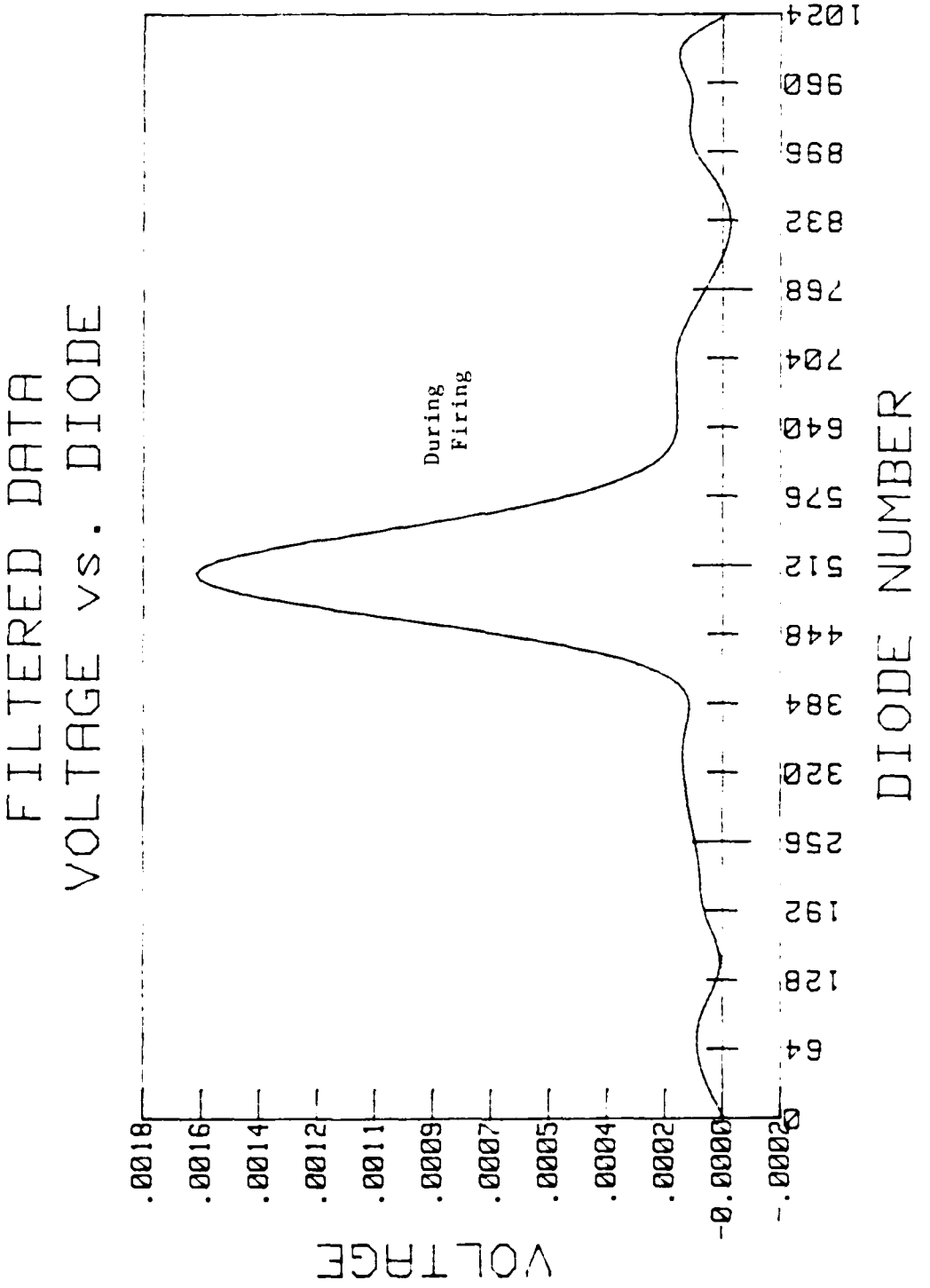


Figure 4.15 Motor Beam Spread Test at Low Pressure

# V. CONCLUSIONS AND RECOMMENDATIONS

Beam wander problems with the motor cavity optical path hampered this investigation. Through a process of elimination it was determined that transient pressure gradients during pressure rise in the motor were bending the beam down several millimeters. This problem may be overcome by taking data during the plateau portion of the propellant burn vice taking data during the pressure rise. Another possible solution might be to raise the array one centimeter above the optical centerline vice dropping it one centimeter. Then the deflected beam would not saturate the array. Perhaps the best solution would be to use a different measuring apparatus for the motor, one in which all of the scattered light would be received on a two-dimensional circular array. The beam fluctuations could then be averaged out.

The modified nitrogen particle injection system showed promise for solving the clogged particle feeder problem.

## LIST OF REFERENCES


1. Air Force Rocket Propulsion Laboratory Interim Report 80-34, Volume 1, A Computer Program for the Prediction of Solid Propellant Rocket Motor Performance, by D. E. Coats, G. R. Nickerson, and R. W. Hermson, et al., April 1981.

2. AIAA Progress in Astronautics and Aerodynamics, Fundamentals of Solid Propellant Combustion, Volume 90, 1975.

3. Buchele, D. R., "Particle Sizing by Measurement of Forward Scattered Light at Two Angles," NASA Technical Paper 2156, May 1983.

4. Horton, K. G., Particulate Sizing in a Solid Propellant Rocket Motor Using Light Scattering Techniques, M.S. Thesis, Naval Postgraduate School, Monterey, California, 1986.

5. Allen, T., Particle Size Measurement, p. 415, Chapman and Hall in association with Methuen, Inc., 1981.

6. Dieck, R. H., and Roberts, R. L., "The Determination of the Sauter Mean Droplet Diameter in Fuel Nozzle Sprays," Applied Optics, September 1970.

7. Dobbins, R. A., Crocco, L., and Glassman, I., "Measurement of Mean Particle Sizes of Sprays from Diffractively Scattered Light," AIAA Journal, Volume 1, No. 8, pp. 1882-1886, 1963.

8. Roberts, J. H., and Webb, M. J., "Measurements of Droplet Size for Wide Range Particle Distributions," AIAA Journal, Volume 2, No. 3, pp. 583, 585, 1964.

9. Mugele, R. A., and Evans, H. D., "Droplet Size Distribution in Sprays," Industrial and Engineering Chemistry, Volume 43, pp. 1317-1324, 1951.

10. Harris, R. K., An Apparatus for Sizing Particulate Matter in Solid Rocket Motors, M. S. Thesis, Naval Postgraduate School, Monterey, California, 1984.

11. Rosa, J. S., Particle Sizing in a Solid Propellant Rocket Motor Using Scattered Light Measurements, M.S. Thesis, Naval Postgraduate School, Monterey, California, 1985.

INITIAL DISTRIBUTION LIST

| | | No. Copies |
|---|---|---|
| 1. | Defense Technical Information Center<br>Cameron Station<br>Alexandria, Virginia 22304-6145 | 2 |
| 2. | Library, Code 0142<br>Naval Postgraduate School<br>Monterey, California 93943-5002 | 2 |
| 3. | Department Chairman, Code 67<br>Department of Aeronautics<br>Naval Postgraduate School<br>Monterey, California 93943-5000 | 1 |
| 4. | Professor D. W. Netzer, Code 67 Nt<br>Department of Aeronautics<br>Naval Postgraduate School<br>Monterey, California 93943-5000 | 2 |
| 5. | LCDR M. G. Keith, USN<br>Naval Air Systems Command, Code PMA-253<br>Washington, D. C. 20361-1253 | 2 |

END

3-87

DTIC